Acta Astronautica 179 (2021) 213–227

Contents lists available at ScienceDirect

Acta Astronautica

journal homepage: www.elsevier.com/locate/actaastro

Satellite equivalence orbits

Ernst Friedrich Mari Jochim [1]

German Aerospace Centre, Oberpfaffenhofen, Germany

ARTICLE INFO

Keywords:
Equivalence orbits
Coupling of satellite motions
Hansen motion
Tropical motion
Meridional motion
Sun-synodic motion
Moon-synodic motion
Molnija similar orbits
Sun-synchronous orbits

ABSTRACT

Satellite **e**quivalence orbits are orbits coupling two or more relative satellite motions. Equivalence orbits between tropical and meridional motion are direct orbits. They have exactly the period 2 sidereal days. As consequence of *Kepler*'s third law the corresponding *Kepler*ian mean semimajor axis is 66931.447 km and gives an impression of this special class of equivalence orbits. In this case the period is identical for all matching orbits and will be preserved by adjusting the orbital elements. Preset 5 orbital elements the sixth element has to be adjusted, e.g. the semimajor axis. The sum of right ascension and geographic longitude shows no secular variations, but only periodic variations due to periodic perturbations, the equation of the center and the reduction on to the equator. The equivalence between tropical and meridional motion offers an independent check of the consistency of the physical parameters. When computed with the *Brouwer* analytical orbit model, the groundtrack of such an equivalence orbit shows no or only small variations over long time intervals. Based on the theory developed, the paper extends the term *equivalent orbits* with respect to *Hansen* motion, anomalistic motion, draconitic motion, Sun-synodic motion, and Moon-synodic motion.

1. Introduction – the saros

The Saros-Cycle corresponds to 223 synodic months or 242 draconitic months. It could be assumed as equivalence as applied to the lunar motion related to the ascending node and the mean Sun. In artificial satellite theory the sunsynchrous orbit is a mostly well-known equivalence orbit. It is equalizing one mean draconitic satellite period to one mean Sun-synodic satellite period. However there exist a huge number of further equivalence orbits with different and highly interesting applications in satellite orbit analysis. The present paper is devoted to the most interesting behavior of some different types of equivalence orbits with respect to meridional motions, Sun-synodic as well as Moon-synodic motions. Different extensions of the term equivalence orbits will be mentioned.

The paper is intended to serve as a supporting tool within early orbit analyses in planned Earth observation as well as planetary orbiter missions.

The motion of a satellite can be described with respect to different reference systems. After a short compilation of these references, various equivalence orbits will be presented in detail. A survey of satellite mean motions and their relations [7] is compiled in Fig. 1.

The paper uses the *Brouwer* [1,10] orbit model including secular, long periodic and short periodic impacts up to the zonal coefficients J_2, J_3,J_4. (The zonal coefficient J_5 will only be respected in the context of special investigations for instance with respect to the frozen eccentricity). The influence of higher orbital impacts, such as higher coefficients of the Earth's gravitational field, including the effects of resonances and commensurabilities, the relation of mass to area of the satellite and its form, mass distribution, attitude control, etc. should be estimated in following investigations. This includes also the time dependent impacts due the varying gravitational attraction from Sun and Moon, the not perfect predictable solar activity with radiation and wind influences on the air drag and the form of the satellite as e.g. the solar panels, gravitational effects of planets, radiation pressure reflected from the Moon, heat emission from the Earth surface on to the satellite, relativistic impacts, impacts due to the Yarkowski-effect, the Poynting-Roberson effect, heat radiation of the satellite antennas and of the satellite body, etc. It will be assumed that all these impacts on a satellite orbit will not obliterate the essential quintessence presented in the paper.

2. Compilation of related satellite motions

A satellite orbit can be characterized by the period with respect to a reference point or reference system. In all cases two different cases of period computation are of interest:

E-mail address: fritz.jochim@dlr.de.
[1] Dr. Ing., retired scientific coworker, e-mail: Fritz.Jochim@dlr.de, DLR Microwave and Radar Institute, Muenchner Str. 20, D-82234 Wessling, Germany.

https://doi.org/10.1016/j.actaastro.2020.10.045
Received 4 March 2020; Received in revised form 10 October 2020; Accepted 25 October 2020
Available online 1 November 2020

Table of symbols

a	semimajor axis [km]
$\overline{a_{QtR}}$	mean semimajor axis of a $(\overline{P_t} \triangleq \overline{P_R})$ – resp. $(P_t \triangleq P_R)$ – equivalence orbit
e	eccentricity
G	equal area parameter [km^2/s] (for conic section orbits: $G = \sqrt{\mu p}$)
i	inclination [deg]
M_0, $\overline{M_0}$	mean anomaly at epoch [deg], mean mean anomaly at epoch [deg]
$(M_0)_s^{\cdot}$	secular variation of mean epoch anomaly [rad/sec]
$\overline{n_a}$, n_a	mean, true anomalistic satellite mean motion [rad/sec]
$\overline{n_d}$, n_d	mean, true draconitic satellite mean motion [rad/sec]
$\overline{n_H}$, n_H	mean, true *Hansen* mean motion [rad/sec]
$\overline{n_L}$, n_L	mean, true Moon-synodic satellite mean motion [rad/sec]
$\overline{n_K}$	*Kepler*ian mean motion [rad/sec]
$\overline{n_P}$, n_P	mean, true planet-synodic satellite mean motion [rad/sec]
n_{Pl}	mean motion of a fictitious mean planet on Earth equator [rad/sec]
$\overline{n_R}$, n_R	mean, true meridional satellite mean motion [rad/sec]
$\overline{n_S}$, n_S	mean, true Sun-synodic satellite mean motion [rad/sec]
$\overline{n_{sid}}$, n_{sid}	mean, true sidereal satellite mean motion [rad/sec]
$\overline{n_t}$, n_t	mean, true tropical motion [rad/sec]
n_O	mean motion of fictitious mean Sun [rad/sec] on Earth equator
n_M	mean motion of fictitious mean Moon [rad/sec] on Earth equator
p	semilatus rectum [km]
p_L	luni-solar precession [arc sec]
$\mathbf{p}_i$	Basic vectors of an inertial system (*Newton* frame) (i = 1,2,3)
P_0	tropical year [d]
$\overline{P_a}$, P_a	mean, true anomalistic period [sec]
$\overline{P_d}$, P_d	mean, true draconitic period [sec]
$\overline{P_H}$, P_H	mean, true *Hansen* period [sec]
$\overline{P_L}$, P_L	mean, true Moon-synodic period
$\overline{P_K}$	mean *Kepler*ian period [sec]
$\overline{P_S}$, P_S	mean, true Sun-synodic period [sec]
$\overline{P_t}$, P_t	mean, true tropical period [sec]
$(\overline{P_t} \triangleq \overline{P_R})$ –	equivalence orbit for coupling between mean tropical and mean meridional satellite motion
$(P_t \triangleq P_R)$ –	equivalence orbit for coupling between true tropical and true meridional satellite motion
Q	Equivalence factor: $\alpha + \lambda = Q = \overline{Q} + \delta Q$, $\overline{Q} = \overline{\alpha} + \overline{\lambda} = \overline{Q}_0 = 2\overline{\Omega}_0 - \Theta_{G0} = \text{const.}$
$\mathbf{q}_j^{(I)}$	Basic vectors of an ideal system (*Hansen* frame) (j = 1,2,3)
r	radius [km]
r_O	geocentric distance of Sun center [km]
r_M	geocentric distance of Moon center [km]
T_U	number of days since fundamental epoch J2000.0 (UT1)
t	time [s] (in universal time UT1)
u	argument of latitude [rad]
V	velocity [km/s]
y_j, $\dot{y}_j$	Cartesian coordinates in $\mathbf{q}_j^{(I)}$-system [km]
α	right ascension of satellite [rad]
α_O	right ascension of Sun [rad]
$\alpha\overline{O}$	right ascension of fictitious mean Sun [rad]
α_2	right ascension of Moon [rad]
ΔJD	difference of date to fundamental epoch J2000.0 in Julian centuries
δ	declination of satellite [rad]
δ_O	declination of Sun [rad]
δ_M	declination of Moon [rad]
δ_p	periodic part of any parameter, e.g. $\alpha = \overline{\alpha} + \delta_p\alpha$
ζ	general orbit angle (first *Hansen* angle) [rad]
η	spatial rotation angle (second *Hansen* angle) [rad]
λ	geographic longitude [rad]
μ, μ_E	gravitational constant of the central body [km^3/s^2]
σ	longitude in orbit of ascending node [rad], related to departure point of *Hansen* system, defined by: $\dot{\sigma} = \dot{\Omega}\cos i$
σ_i	retrograde factor: $\sigma_i = \text{sgn}(\cos i)$
$\overline{\tau}$, τ	mean, true solar angle of satellite [rad]: $\tau = \alpha - \alpha_O$, $\overline{\tau} = \alpha - \alpha_{\overline{O}}$
$\overline{\tau_M}$, τ_M	mean, true Moon angle [rad]: $\tau_M = \alpha - \alpha_M$, $\overline{\tau_M} = \alpha - \alpha_{\overline{M}}$
Θ_G	sidereal time at Greenwich meridian [deg]
Θ_{G0}	sidereal time at midnight Greenwich meridian [deg]
$\dot{\Theta}$	tropical rotational rate of Earth [rad/sec]
υ	true anomaly [deg]
ω	argument of perigee [deg]
$\dot{\omega}_s$	secular variation of argument of perigee [rad/s]
Ω	right ascension of ascending node [deg]
$\dot{\Omega}_s$	secular variation of right ascension of ascending node [rad/s]

1. Mean periods based on the mean satellite motion using mean orbital elements at epoch, such as the *Kepler*ian elements, e.g.

$$\overline{P} = 2\pi \ / \overline{n}, \overline{n} = fct\left(\overline{a}_0,\ \overline{e}_0, \overline{i}_0, \overline{\Omega}_0, \overline{\omega}_0, \overline{M}_{00}\right) \tag{2.1}$$

2. A more realistic approach is the computation of a satellite period by using an analytical or numerical ephemeris over one or more periods. Let the reference to a certain relation be characterized by a certain orbit angle x. A period P will be calculated by the change of the orbital angle by $2N\pi$ using a condition function of the form e.g.

$$fct[P(t_0)] \equiv \sin[x(t_0 + N\,P) - x(t_0)] = 0 \ \langle N \text{ integer number.}. \tag{2.2}$$

Instead of calculating the angles x directly, this kind of condition function uses the sinus function as a superposed function [12] which allows a smooth and stable computation, avoiding the error-prone change of the angles in the vicinity of $2N\pi$. The value of the period will not only be a function of the orbit relation but also of the epoch t_0.

2.1. Keplerian and Hansen motion

The period of an unperturbed *Kepler*ian motion can be calculated using the general formula of *Kepler*'s third law

$$P_K = 2\pi\,/n_K = 2\pi\,a\,\sqrt{a/\mu}. \tag{2.3}$$

This motion uses the true υ or eccentric anomaly as orbital angle. In the so-called perturbed case the reference of these angles is the apsidal line which is moving due to orbital perturbations. The only system avoiding a proper motion within the orbital system was found by *P. A. Hansen* [1,2,5,6], and [9]. This system is based on to a fixed starting point within the orbital plane, called "departure point". The orbital angle ζ of such a *Hansen*-system is defined by *Kepler*'s law of areas with equal area parameter G

$$\dot{\zeta} = G/r^2, \zeta = \zeta_0 + \int_{t_0}^{t} G/r^2 \; dt \tag{2.4}$$

Starting at the departure point an angle σ along the orbital plane will intersect the equatorial plane at the ascending node. If the argument of latitude u is known by an ephemeris computation, the orbital angle can be computed from [7].

$$\zeta = u + \sigma = \upsilon + \omega + \sigma. \tag{2.5}$$

The nodal angle σ is only defined by its differential equation $\dot{\sigma} = \dot{\Omega}\cos i$, so that

$$\zeta = \upsilon + \omega + \int_{t_0}^{t} \dot{\sigma}\,\mathrm{dt} = \upsilon + \omega + \int_{t_0}^{t} \dot{\Omega}\cos i \; dt\,. \tag{2.6}$$

Its variation is

$$\dot{\zeta} = \dot{\upsilon} + \dot{\omega} + \dot{\Omega}\cos i = \dot{u} + \dot{\sigma}. \tag{2.7}$$

From this relationship the mean *Hansen* mean motion and the mean *Hansen* period will be obtained

$$\overline{n_H} := \dot{\bar{\zeta}} = \overline{n_K} + (M_0)_s^{\cdot} + \dot{\omega}_s + \dot{\Omega}_s \cos\bar{i}_0, \overline{P_H} := 2\pi / \overline{n_H}. \tag{2.8}$$

For the expressions of the secular variations $[(M_0)_s^{\cdot},\ \dot{\omega}_s,\ \dot{\Omega}_s]$ see e.g. in Refs. [1]. In practical applications the inclination is quite stable, so that

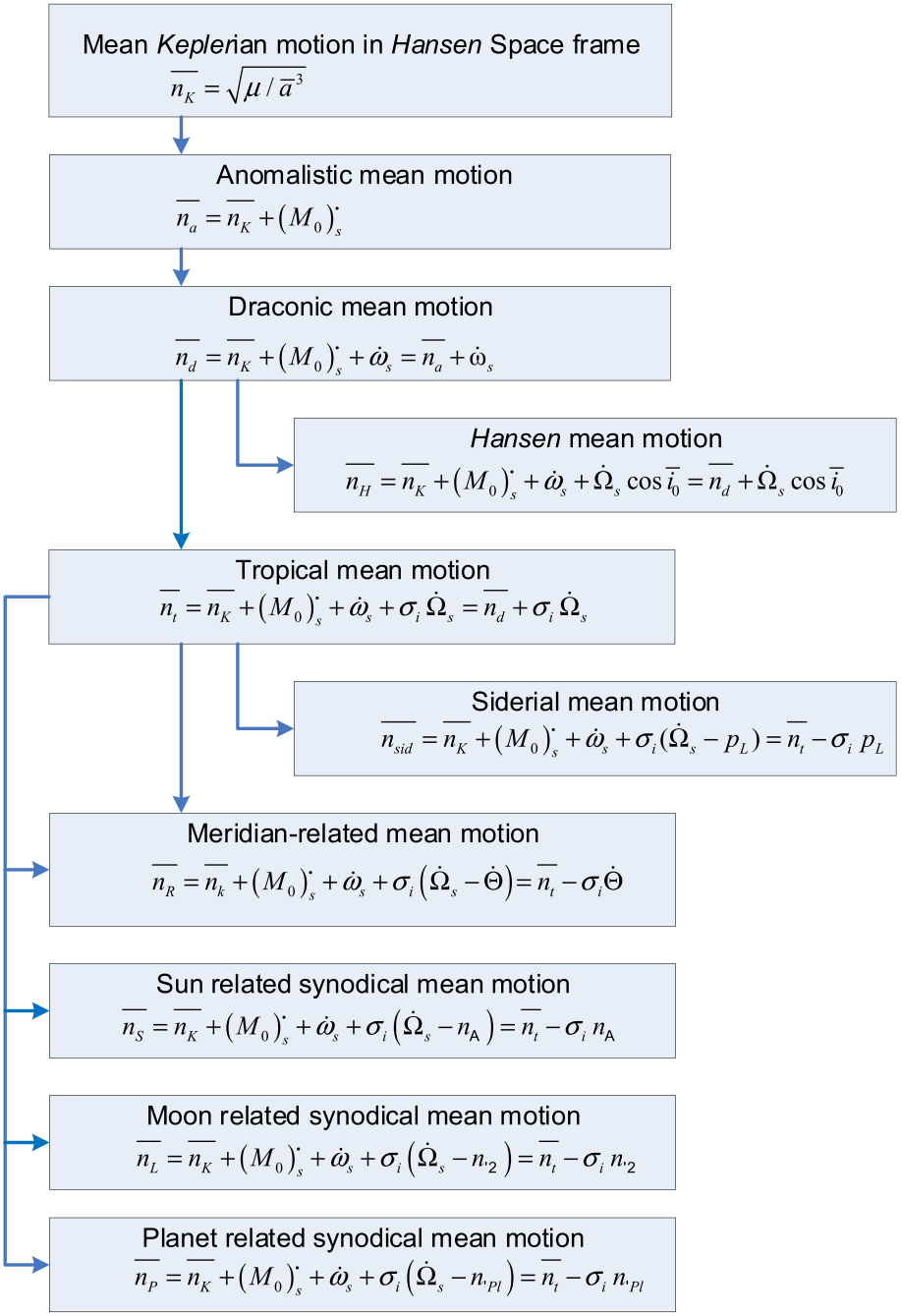

Fig. 1. Survey on satellite mean motion with respect to different reference systems.

$\cos i$ may be replaced by a constant factor $\cos\bar{i}_0$. Selecting an initial value for ζ_0 at epoch t_0 and computing the argument of latitude $u_0 = u(t_0)$, the initial value

$$\sigma_0 = \zeta_0 - u_0 \tag{2.9}$$

will be obtained. Through the separation of the right ascension of the ascending node into a secular and a periodic part

$$\Delta\Omega := \dot{\Omega}_s\ (t - t_0) + \delta\Omega[t, t_0], \tag{2.10}$$

the integral in (2.6) can finally be replaced by

$$\zeta = \zeta(t) = \sigma_0 + u + \Delta\Omega\cos\bar{i}_0\ + \cdots. \tag{2.11}$$

The (true) *Hansen* period can be computed for pre-set orbital elements using the superposed condition function

$$fct[P_H(t_0)] \equiv \sin[\zeta(t_0 + P_H) - \zeta(t_0)] = 0. \tag{2.12}$$

For the iterative solution the mean *Kepler*ian period (2.3) with epoch value $\overline{a}_0$ can be used as a first approximation.

2.2. Anomalistic motion

The anomalistic satellite motion is related to the line of apsides. Reference point is usually the perigee. The true anomaly υ will be used as orbital angle of the anomalistic motion.

With application of the equation of center the mean anomalistic motion and the mean anomalistic period will be obtained

$$\overline{n_a} = \overline{n_K} + (M_0)^{\cdot}_s, \quad \overline{P_a} = 2\pi/\overline{n_a} \tag{2.13}$$

Independent from this mean period, the true anomalistic period $P_a$can be computed iteratively with an analytic or numerical ephemeris using the condition function

$$fct[P_a(t_0)] \equiv \sin[\upsilon(t_0 + P_a) - \upsilon(t_0)] = 0. \tag{2.14}$$

As a first approximation the mean *Kepler*ian period (2.3) or the mean anomalistic period (2.13) can be used.

2.3. Draconitic motion

The satellite draconitic motion is related to the nodal line. Usually the ascending node will be selected as reference point. The orbital angle is the argument of latitude $u = \upsilon + \omega$. The mean draconitic mean motion and the mean draconitic period[2] will be computed from

$$\overline{n_d} = \overline{n_K} + (M_0)^{\cdot}_s + \dot{\omega}_s = \overline{n_a} + \dot{\omega}_s, \overline{P_d} = 2\pi / \overline{n_d}. \tag{2.15}$$

Independently the true draconitic period P_d can be computed by means of the superposed condition function

$$fct[P_d(t_0)] \equiv \sin[u(t_0 + P_d) - u(t_0)] = 0. \tag{2.16}$$

Starting value for the iteration might be the mean *Kepler*ian or the mean draconitic period.

[2] In English literature sometimes erroneously the term „nodal period" will be used instead of „draconitic period"

2.4. Tropical motion

The tropical motion relates a satellite motion to the vernal equinox. Therefore the basic plane to investigate the tropical motion is the Earth equatorial plane. It is custom to use the "bending angle" $l := \Omega + u$ as an orbital angle within the tropical motion. However in the present application the period of the satellite with respect to the vernal equinox is of interest. In this respect, the right ascension could be used as orbital angle instead. Then the true tropical period can be computed using the condition function

$$fct[P_t(t_0)] \equiv \sin[\alpha(t_0 + P_t) - \alpha(t_0)] = 0. \tag{2.17}$$

The iteration process can be started again with the mean *Kepler*ian period or with the mean tropical period as developed in the following section.

Two steps will be necessary to derive the formula for the mean tropical motion. The first step is the use of the equation of center.

The second step is the reduction to the equator [3,4,7]. The part of the orbit with respect to the ascending node will be projected down to the equator. In order to get a unique formulation the right ascension with respect to the node will be introduced using the retrograde factor $\sigma_i := \mathrm{sgn}\ (\cos i)$:

$$\alpha_N := \sigma_i\ (\alpha - \Omega) \tag{2.18}$$

Using $\sigma_i = \mathrm{sgn}(\dot{\alpha})$ from $\dot{\alpha} = \dot{\zeta}\cos i\ /\cos^2\delta$ the derivation finally leads to the segmentation of $\dot{\alpha}$ into a secular and a periodic part [7].

$$\sigma_i\ \dot{\alpha} = \sigma_i\ (\dot{\bar{\alpha}} + \delta_P\dot{\alpha}) = \sigma_i\ \dot{\Omega}_s\ + \overline{n_K}_0 + (M_0)^{\cdot}_{s0} + \dot{\omega}_{s0} + \sigma_i\ \delta_P\dot{\alpha} > 0. \tag{2.19}$$

The secular part assumed as the mean tropical mean motion and correspondingly the mean tropical period can be written as

$$\overline{n_t} := \sigma_i\ \dot{\bar{\alpha}} = \overline{n_K}\ + (M_0)^{\cdot}_s + \dot{\omega}_s + \sigma_i\ \dot{\Omega}_s = \overline{n_d}\ + \sigma_i\ \dot{\Omega}_s,\ \overline{P_t} = 2\pi\ /\ \overline{n_t}. \tag{2.20}$$

2.5. Meridional Motion

For the comparison of the different relations of satellite motion, the tropical motion is of central importance. This will be shown at first in the case of the meridional (meridian-related) motion. This motion relates to the 0-Meridian ("Greenwich-Meridian") of the Earth's geographic coordinate system. However the geographic longitude λ is directly related to the vernal equinox by means of the sidereal time Θ_G at Greenwich meridian via the relation [8,11].

$$\begin{aligned} &\alpha = \Theta_G + \lambda, \Theta_G = \Theta_{G_0} + \dot{\Theta}\ t \\ &\dot{\Theta} = 1.002737909350795 + 5.9006 \times 10^{-11}\ \ T_U + 5.9 \times 10^{-15}\ \ T_U^2\ \text{[periods per mean solar day]} \end{aligned} \tag{2.21}$$

Θ_{G0} is the sidereal time at midnight Greenwich, t the solar time (UT1), T_U the number of days since fundamental epoch J2000.0 (UT1). The geographic longitude λ serves as an orbital angle within the meridional motion. λ defines the meridian to which the motion is related. Using the derivation of the variation of the right ascension (2.19) we get the segmentation into a secular and a periodic part

$$\sigma_i\ \dot{\lambda} = \sigma_i\ \dot{\bar{\lambda}} + \sigma_i\ \delta\dot{\lambda} = \sigma_i\ \dot{\bar{\alpha}} - \sigma_i\ \dot{\Theta} + \sigma_i\ \delta\dot{\lambda} = \overline{n_K} + (M_0)^{\cdot}_s + \dot{\omega}_s + \sigma_i\left(\dot{\Omega}_s - \dot{\Theta}\right) + \sigma_i\delta_p. \tag{2.22}$$

From this expression the mean meridional mean motion and the mean meridional period can be obtained

$$\overline{n_R} := \sigma_i\ \dot{\bar{\lambda}}\ = \overline{n_K} + (M_0)^{\cdot}_s + \dot{\omega}_s + \sigma_i\left(\dot{\Omega}_s - \dot{\Theta}\right) = \overline{n_t} - \sigma_i\ \dot{\Theta}, \overline{P_R} = 2\pi\ /\ \overline{n_R}. \tag{2.23}$$

This expression shows that for retrograde orbits the mean meridional motion is always positive. However for direct orbits the mean meridional motion might vanish or could be negative if $\overline{n_t} \leq \dot{\Theta}$. By this remarkable behavior the meridional motion is different from all other related motions.

Using the geographic longitude as orbital angle of the meridional motion, the true meridional period can be computed by means of the condition function

$$fct[P_R(t_0)] \equiv \sin[\lambda(t_0 + P_R) - \lambda(t_0)] = 0. \tag{2.24}$$

2.6. Sun-synodic motion

The expression describing satellite motion relative to the Sun is based on two different definitions of the Sun's motion. At first, the true Sun is well known at any time point by an ephemeris producing the equatorial polar coordinates $r_0(\alpha_0,\ \delta_0)$. The tropical period of the Sun is a tropical year P_0 with mean motion (see e.g. Refs. [8,11] ch. 6.8)

$$n_0 = 2\pi\ /\ P_0\ = 0.00273790093\ [\text{periods}\ /\ \text{d}]\ + \cdots. \tag{2.25}$$

It is connected to the tropical rotation of the Earth by

$$n_0 = \dot{\Theta} - 1\ [\text{periods}\ /\ \text{d}]\ =\ \dot{\Theta} - 2\pi\ /\ 86400\ [1\ /\ s]. \tag{2.26}$$

A fictitious mean Sun will be defined with the same period P_0 as the true Sun, but moving with uniform motion n_0 along the Earth's equator. The motion of the fictitious mean Sun will be obtained from the true Sun by combined application of the equation of the center and the reduction to the equator. Its right ascension will be computed related to an initial value $\alpha_{\overline{\odot}0}$ by

$$\alpha_{\overline{\odot}} = \alpha_{\overline{\odot}0} + n_0\ (t - t_0). \tag{2.27}$$

The link of the true Sun to the satellite's motion will be obtained by the solar angle

$$\tau := \alpha - \alpha_{\odot}. \tag{2.28}$$

Then the Sun-related satellite motion has the true period P_S from

$$fct[P_S(t_0)] \equiv \sin[\tau(t_0 + P_S) - \tau(t_0)] = 0. \tag{2.29}$$

The iteration process starts with the mean *Kepler*ian period or the mean Sun-related period as computed below

$$P_S^{(0)} = \overline{P_K} \text{ or } P_S^{(0)} = \overline{P_S}. \tag{2.30}$$

In order to compute the mean Sun-related mean motion the mean solar angle will be defined with respect to the fictitious mean Sun

$$\overline{\tau} := \alpha - \alpha_{\overline{\odot}}. \tag{2.31}$$

Similar to the derivation of the mean meridional motion (2.22) we get the segmentation into a secular and a periodic part δ_P.

$$\sigma_i\,\dot{\overline{\tau}} = \sigma_i\left(\dot{\overline{\tau}}_s + \dot{\delta\overline{\tau}}\right) = \sigma_i\,\dot{\overline{\alpha}} - \sigma_i\,n_0 + \sigma_i\,\dot{\delta\overline{\tau}} = \overline{n_K} + (M_0)_s^{\cdot} + \dot{\omega}_s + \sigma_i\left(\dot{\Omega}_s - n_0\right) + \sigma_i\dot{\delta}_p \tag{2.32}$$

The secular part leads to the mean Sun-related mean motion

$$\overline{n_S} := \sigma_i\,\dot{\overline{\tau}}\ = \overline{n_K} + (M_0)_s^{\cdot} + \dot{\omega}_s + \sigma_i\left(\dot{\Omega}_s - n_0\right) = \overline{n_t} - \sigma_i\,n_0 \tag{2.33}$$

and the mean satellite period with respect to the fictitious mean Sun

$$\overline{P_S} = 2\pi\ /\ \overline{n_S} = 2\pi\ /\ \left[\overline{n_K}\ +\ (M_0)_s^{\cdot} + \dot{\omega}_s + \sigma_i\left(\dot{\Omega}_s - n_{\text{A}}\right)\right]. \tag{2.34}$$

2.7 Moon-synodic motion

The motion of the Moon when mathematically described as moving around the Earth can also be of interest for the analysis of Earth satellite motion. It can be studied similarly to the relation of a satellite motion with respect to the rotating Earth surface as well as to the relative motion of the Sun. Therefore a Moon-synodic motion of an Earth satellite might also be inspected.

The link between the different kinds of satellite motion is computed along the Earth equator. If the equatorial polar coordinates of the Moon center $r_2(\alpha_2,\ \delta_2)$ are known from a lunar ephemeris a true Moon angle

$$\tau_M = \alpha - \alpha_M \tag{2.35}$$

can be introduced. The true Moon-synodic satellite period P_L can be computed using the superposed condition function

$$fct[P_L(t_0)] \equiv \sin[\tau_2(t_0 + P_L) - \tau_2(t_0)] = 0. \tag{2.36}$$

A first approximation for the iterative solution could be the mean *Kepler*ian period or a mean Moon-synodic period as derived in the following.

Similarly to the Sun a fictitious mean Moon might be derived. It will be computed with the equation of the center and the reduction to the equator. This fictitious mean Moon has the same period i.e. the tropical month around the Earth as the true Moon. Its tropical mean motion [8, 11]

$$\begin{aligned} n_{\text{M}} = \ & 13^{\circ}.176396476\ -\ 1^{\circ}.2080799 \times 10^{-12}\ (\Delta JD)[1/\text{d}] + \\ & 1^{\circ}.083101 \times 10^{-19}\ (\Delta JD)^2\ \left[1/\text{d}^2\right] + \ \cdots\ [1/\text{d}] \end{aligned} \tag{2.37}$$

shows small deviations which can be neglected in the frame of satellite orbit analysis (ΔJD is the difference of date to the fundamental epoch J2000.0 in Julian centuries). The fictitious mean Moon can be defined by

$$\alpha_{\overline{M}} = \alpha_{\overline{M}0} + n_M\ (t - t_0) \tag{2.38}$$

and a mean Moon-satellite-angle by

$$\tau_{\overline{M}} := \alpha - \alpha_{\overline{M}}. \tag{2.39}$$

Similarly to the Sun relation in formulae (2.33) we get for the mean Moon-synodic satellite mean motion

$$\overline{n_L} := \sigma_i\,\dot{\overline{\tau_M}}\ = \overline{n_K} + (M_0)_s^{\cdot} + \dot{\omega}_s + \sigma_i\left(\dot{\Omega}_s - n_M\right) = \overline{n_t} - \sigma_i\,n_M \tag{2.40}$$

and the mean Moon-related satellite period

$$\overline{P_L} = 2\pi\ /\overline{n_L} = 2\pi\ /\ \left[\overline{n_K}\ +\ (M_0)_s^{\cdot} + \dot{\omega}_s + \sigma_i\left(\dot{\Omega}_s - n_M\right)\right] \tag{2.41}$$

3. Equivalence satellite orbits related to meridional motion

In comparison with other related satellite motions, the meridional satellite motion is of a very special character. The consideration of oversynchronous orbits leads to some surprising insights about satellite orbit behavior with interesting consequences.

3.1. Direct oversynchronous satellite orbits

The considerations in this chapter are based on the relationship (2.23) $\overline{n_R} = \overline{n_t} - \sigma_i\,\dot{\Theta}$.

In case of retrograde orbits $[\sigma_i = \text{sgn}(\cos i) = -1]$ the mean meridional mean motion is always positive: $\overline{n_R}(\sigma_i = -1) > 0$. For direct orbits $[\sigma_i = \text{sgn}(\cos i) = +1]$ however, if the mean tropical mean motion is smaller than the mean tropical Earth rotational rate $\overline{n_t} < \dot{\Theta}$, it follows $\overline{n_R} < 0$ and therefore

$$\overline{n_R} < 0 < \overline{n_t} < \dot{\Theta}\ \langle\sigma_i = +1\ ,\ \overline{n_t} < \dot{\Theta}. \tag{3.1}$$

Formula (2.23) shows analogously

$$\dot{\overline{\lambda}} = \dot{\overline{\lambda}}[\sigma_i = 1,\ \overline{n_t} < \dot{\Theta}] = \overline{n_R} = \overline{n_t} - \dot{\Theta} < 0, \tag{3.2}$$

that the satellite seems to move backwards whereas its true motion is direct.

As seen in Fig. 2 three cases have to be distinguished:

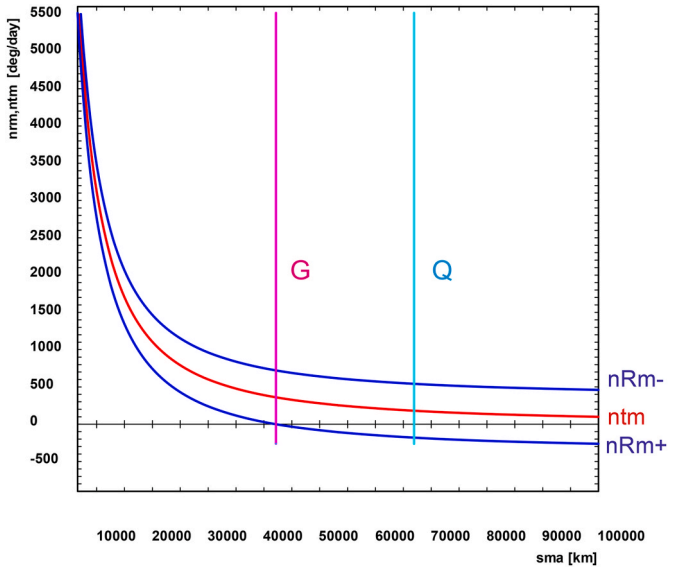

Fig. 2. Comparison of the mean tropical mean motion (ntm) with the mean meridional mean motion (nRm+) for direct orbits and (nRm-) for retrograde orbits versus the semimajor axis of a satellite orbit. „G" characterizes the geosynchronous orbit, „Q" the equivalence between tropical and Meridian-related mean motion.

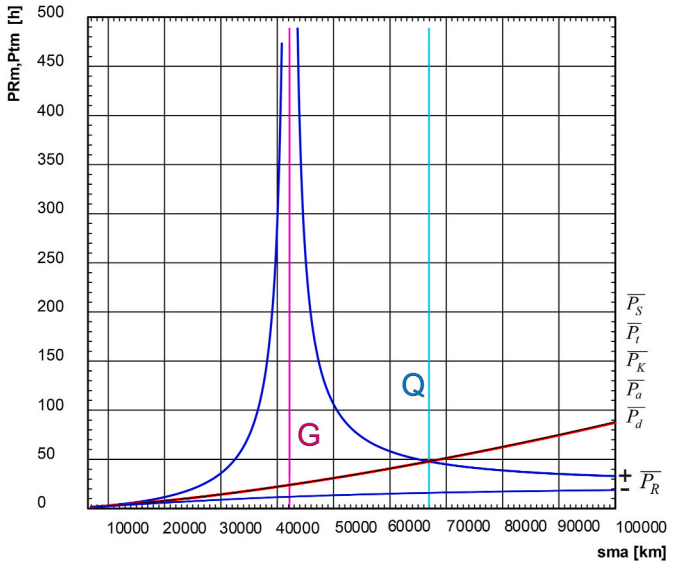

Fig. 3. Comparison of the mean meridional period $\overline{P_R}$ (blue curves) against other mean periods (red and black curve) versus the semimajor axis for direct (+) and retrograde (−) orbits. The resolution of the figure is too coarse to show the difference between the draconitic, anomalistic, tropical, *Kepler*ian period, whereas the Sun-synodic period (black) shows minimal deviations with respect to the other periods. „G" characterizes the geosynchronous orbit, „Q" the equivalence of tropical and meridional period for the mean semimajor axis $\overline{a_{QK}} = 66932.768$ km(*Kepler*ian „equivalence-orbit"). The computation of the curves with semimajor axis as independent variable uses the *Kepler*ian mean elements $\overline{e}_0 = 0.5, \overline{i}_0 = 50°, \overline{\Omega}_0 = \overline{\omega}_0 = 0°, \overline{M_{00}} = 180°$ for the direct orbit, the retrograde orbit uses the inclination $\overline{i}_0 = 110°$. (For interpretation of the references to color in this figure legend, the reader is referred to the Web version of this article.)

1. If the value of the mean meridional mean motion is smaller than the mean tropical mean motion, then the mean meridional period must be greater than the mean tropical period

$$\overline{P_R} > \overline{P_t} \qquad \langle \sigma_i = +1, \overline{n_t} < \dot{\Theta},\ |\overline{n_R}| < \overline{n_t}. \tag{3.3}$$

After a period, the projection of a satellite position onto the equator will intersect the same right ascension before the same geographic longitude. Correspondingly the other periods will be smaller than the meridional period

$$\overline{P_K} < \overline{P_R}, \overline{P_H} < \overline{P_R},\ \overline{P_a} < \overline{P_R},\ \overline{P_d} < \overline{P_R}\ \langle \sigma_i = +1\ ,\ \overline{n_t} < \dot{\Theta},\ |\overline{n_R}| < \overline{n_t}. \tag{3.4}$$

2. If the value of the mean meridional mean motion is greater than the mean tropical mean motion, then the mean meridional period is smaller than the mean tropical period

$$|\overline{n_R}| > \overline{n_t} \Leftrightarrow \overline{P_R} < \overline{P_t}\ \langle \mathrm{sgn}(\cos i = +1)\ ,\ \overline{n_t} < \dot{\Theta}, \tag{3.5}$$

a satellite will intersect the geographical longitude before the corresponding right ascension. Correspondingly the other periods will be greater than the meridional period

$$\overline{P_K} > \overline{P_R},\ \overline{P_H} > \overline{P_R},\ \overline{P_a} > \overline{P_R},\ \overline{P_d} > \overline{P_R}\ \ \langle \sigma_i = +1\ ,\ \overline{n_t} < \dot{\Theta},\ |\overline{n_R}| > \overline{n_t}. \tag{3.6}$$

3. The point where the value of the mean tropical motion is identical to the mean meridional motion is of special interest:

$$|\overline{n_R}| = \overline{n_t} \Leftrightarrow \overline{P_R} = \overline{P_t}\ \langle\ \overline{n_t} < \dot{\Theta}\ . \tag{3.7}$$

It is presented in Fig. 3 as the intersection point of the curves of the meridional period and the tropical (as well as other) periods. This point corresponds to the semimajor axis which is characterized by the line "Q". Because of the equivalence of the two periods in this point, we propose to call the corresponding satellite orbit with semimajor axis "Q" an "*equivalence orbit*".

This concept gives cause to investigate e.g.

- ➢ if there are special features of equivalence orbits,
- ➢ if there are other equivalence orbits not restricted to meridional periods,
- ➢ if the term equivalence orbits be generalized,
- ➢ if equivalence orbits exist not only for mean but also for true satellite motions,
- ➢ if multiple equivalences exist,
- ➢ if there are any restrictions for equivalence orbits.

In order to characterize equivalence orbits unambiguously we introduce the following notation:

$(\overline{P_t} \triangleq \overline{P_R})-$ equivalence orbit for coupling between mean tropical and mean meridional periods

$(P_t \triangleq P_R)-$ equivalence orbit for coupling between true tropical and true meridional periods.

3.2. Coupling of tropical and meridional motion

3.2.1. Basic characteristics

Between mean tropical and mean meridional motions in case of equivalence the relationship exists (see Figs. 3–1)

$$\overline{n_R} = -\overline{n_t}. \tag{3.8}$$

With this, formula (3.2) yields

$$|\overline{n_R}| = \overline{n_t} = \dot{\Theta}/2. \tag{3.9}$$

This allows the computation of the value of the corresponding mean periods with

$$\overline{P_R} = \overline{P_t} = 4\pi \ / \dot{\Theta}. \tag{3.10}$$

Using the tropical rotational rate $\dot{\Theta}$ of the Earth's rotation from (2.21) we can derive the period of a $(\overline{P_t} \triangleq \overline{P_R})-$ equivalence orbit

$$\overline{P_{RQ}} = \overline{P_{tQ}} = 4\pi \ / \dot{\Theta} = 172328.1811 \text{ s} \triangleq 47^h 52^m 08^s.1811. \tag{3.11}$$

This is exactly the value of two sidereal days. As an essential result we can conclude:

The period of a $(\overline{P_t} \triangleq \overline{P_R})-$ equivalence orbit is independent from any orbital elements.

The corresponding mean semimajor axis can be computed by adaption of *Kepler*'s third law

$$\overline{a_{QK}} = \sqrt[3]{4\mu/\dot{\Theta}^2} = 66931.4468893 \text{ km}. \tag{3.12}$$

This value is valid in the case of a so-called „unperturbed" *Kepler*ian orbit. In the usual case of physical disturbances on the orbits ("perturbed *Kepler*ian orbits") a suitable orbit model has to be used. Applying this model the mean semimajor axis $\overline{a_Q}$ of such an equivalence orbit usually must be computed iteratively. If the other orbital parameters, e.g. the mean *Kepler*ian elements eccentricity $\overline{e}_0$ and inclination $\overline{i}_0$ are known at any epoch t_0, and if a first order approximation of the semimajor axis is also known, for instance from (3.12), the mean periods can be obtained from (2.20) and (2.23). Then the condition function

$$fct\left(\overline{a_{QtR_0}}\right) \equiv \overline{P_R} - \overline{P_t} = 0 \ \langle \overline{P_R} = 2\pi \ / \overline{n_R} \ , \ \overline{P_t} = 2\pi \ / \overline{n_t} \tag{3.13}$$

allows the computation of the mean semimajor axis related to the epoch.

Similarly as for mean motions an analog representation can be defined for true motions: The semimajor axis of a $(P_t \triangleq P_R)-$ equivalence orbit can be obtained by an iterative solution of the condition function

$$fct\left(\overline{a_{QtR_0}}\right) \equiv P_t - P_R = 0, \tag{3.14}$$

where at each step the true periods must iteratively be computed with (2.17) and (2.24) with the semimajor axis as independent variable:

$$fct[P_t(t_0)] \equiv \sin[\alpha(t_0 + P_t) - \alpha(t_0)] = 0; fct[P_R(t_0)] \equiv \sin[\lambda(t_0 + P_R) - \lambda(t_0)] = 0. \tag{3.15}$$

The whole process (3.14)–(3.15) has to be repeated. The accuracy condition will usually be selected for $fct(\overline{a_{QtR}})$. The value (3.12) can be selected as initial value for the semimajor axis. The iteration process is usually numerically very stable.

If an analytical orbit propagator (e.g. Ref. [1,10]) is used, the mean semimajor axis has to be selected by the iteration process (3.13) or (3.14)–(3.15), either with respect to the mean or the true equivalence orbits. This computation will not only be affected by the equivalence condition but also essentially by the remaining 4 *Kepler*ian parameters $(\overline{e}_0, \ \overline{i}_0, \ \overline{\omega}_0, \ \overline{M_{00}})$.

The result is shown in Table 1 for different eccentricities and inclinations as well as in Table 1 for some different right ascensions of the node $\overline{\Omega}_0$, arguments of perigee $\overline{\omega}_0$ and mean mean anomaly at epoch $\overline{M_{00}}$. The periods of the $(\overline{P_t} \triangleq \overline{P_R})-$ equivalence orbits are identical in all different cases of the elements and are nearly matching with the theoretical value obtained in formula (3.11). This fact also holds true in case of a $(P_t \triangleq P_R)-$ equivalence. This fixed period time will slightly differ if

Table 2
Computation of the semimajor of a $(P_t \triangleq P_R)-$ equivalence orbit with eccentricity $\overline{e}_0 = 0.9$ and inclination $\overline{i}_0 = 85°$, for different orbit parameters $\overline{\Omega}, \overline{\omega}, \overline{M_0}$, at epoch: 2019-10-12/00:00:0.00, basic geodetic parameters: $R_E = 6378.1366$ km, $\mu_E = 398600.4418 \text{ km}^3/\text{s}^2$, $\dot{\Theta} = 0.72921158573340 \times 10^{-4}$ /s.

$\overline{a_{Qt}}$	$\overline{e}_0$	$\overline{i}_0$	$\overline{\Omega}_0$	$\overline{\omega}_0$	M_0	$P_{t,\text{sec}} = P_{R,\text{sec}}$
66926.947442 km	0.9	85°	0°	0°	0°	172328.181014 s
66777.137561 km	0.9	85°	0°	0°	90°	172328.181014 s
66777.137561 km	0.9	85°	120°	0°	90°	172328.181014 s
66829.750982 km	0.9	85°	120°	60°	90°	172328.181014 s
66867.160953 km	0.9	85°	120°	120°	90°	172328.181014 s
66827.647918 km	0.9	85°	120°	120°	150°	172328.181014 s
66702.550233 km	0.9	85°	0°	0°	180°	172328.181014 s
66702.550233 km	0.9	85°	150°	180°	180°	172328.181014 s
66816.076386 km	0.9	85°	120°	60°	180°	172328.181014 s
66815.840898 km	0.9	85°	120°	60°	120°	172328.181014 s

Note 2: Due to the great height of the semimajor axis in the case of equivalence between tropical and meridional motion high eccentric orbits can be of special interest for some remote sensing tasks. If for instance the perigee height is desired in the range of 300 km, of course the orbit will be affected significantly by the air drag as consequence of the solar flux. However this only can be investigated in a second step of orbit analysis with respect to a special launch date, satellite form (e.g. ratio mass to area, orientation of solar cells, distribution of mass inside the satellite) etc. This cannot be the task within the frame of a general satellite orbit analysis as discussed in the present paper.

Table 1
Computation of the semimajor axis of a $(\overline{P_t} \triangleq \overline{P_R})-$ and a $(P_t \triangleq P_R)-$ equivalence orbit based on different eccentricities and inclinations, $\overline{\Omega} = \overline{\omega} = \overline{M_0} = 0$, epoch: 2019-10-16/12:00:0.00, basic parameters: $R_E = 6378.1366$ km, $\mu_E = 398600.4418 \text{ km}^3/\text{s}^2$, $\dot{\Theta} = 0.72921158573340 \times 10^{-4}$ /s.

$\overline{e}_0$	$\overline{i}_0$	$\overline{a_{Qt}}[\overline{P_t} \triangleq \overline{P_R}]$	$\overline{P_t} = \overline{P_R}$	$\overline{a_{Qt}}[P_t \triangleq P_R]$	$P_{t,\text{sec}} = P_{R,\text{sec}}$
0.0	0°	66932.763262 km	172328.181014	66932.763262 km	172328.181014 s
	30°	66932.193394 km	172328.181014	66932.105237 km	172328.181014 s
	60°	66931.118205 km	172328.181014	66930.789190 km	172328.181014 s
	85°	66930.751846 km	172328.181014	66930.151162 km	172328.181014 s
0.3	0°	66932.999861 km	172328.181014	66932.613406 km	172328.181014 s
	30°	66932.325413 km	172328.181014	66932.074037 km	172328.181014 s
	60°	66931.054479 km	172328.181014	66930.995323 km	172328.181014 s
	85°	66930.625382 km	172328.181014	66930.472364 km	172328.181014 s
0.5	0°	66933.630186 km	172328.181014	66932.798039 km	172328.181014 s
	30°	66932.675807 km	172328.181014	66932.207038 km	172328.181014 s
	60°	66930.881878 km	172328.181014	66931.025093 km	172328.181014 s
	85°	66930.287582 km	172328.181014	66930.451205 km	172328.181014 s
0.8	0°	66939.573455 km	172328.181014	66934.832848 km	172328.181014 s
	30°	66935.935768 km	172328.181014	66933.478288 km	172328.181014 s
	60°	66929.161745 km	172328.181014	66930.770120 km	172328.181014 s
	85°	66927.074292 km	172328.181014	66929.457636 km	172328.181014 s
0.9	0°	66957.658059 km	172328.181014	66939.818714 km	172328.181014 s
	30°	66945.695786 km	172328.181014	66936.571570 km	172328.181014 s
	60°	66923.609455 km	172328.181014	66930.086768 km	172328.181014 s
	85°	66917.213816 km	172328.181014	66926.947442 km	172328.181014 s

modified astronomic parameters are used and if any other epoch will be chosen. It should be noted that each computation is done independently. The required accuracy was 10^{-8} sec.

If an equivalence orbit is not referred to the perigee but to any other position in a satellite orbit the selection of the semimajor axis will be influenced strongly. In Table 2 $(P_t \triangleq P_R)-$ equivalence orbits with eccentricity e = 0.9 are investigated for example. The importance of such an orbit is the perigee height $H_P \approx 316$ km, which might be of useful for special observations. The satellite passes the perigee with the velocity $V_P \approx 10.6$ km/s. The apogee height is $H_A \approx 128000$ km. Also in this extreme case the periods presented in the table are again all identical with respect to the same epoch and again nearly matching with the value (3.11).

Note 1: The periods computed in Table 1 can differ from the correct value computed in formula (3.11). The deviation can be caused by the inconsistence of the astronomical parameters. Therefore to check the consistency of a set of basic parameters, the computation of a $(\overline{P_t} \triangleq \overline{P_R})-$ and/or a $(P_t \triangleq P_R)-$ equivalence orbit can be essentially helpful.

3.2.2. Further general characteristics

1. Using the general relationships (2.19) and (2.22), based on the condition for direct orbits $(\sigma_i = +1)$, on the condition for oversynchronous orbits (3.1) $[\overline{n_R} < 0 < \overline{n_t} < \dot{\Theta}]$ as well as on the necessary and sufficient condition (3.8) for $(\overline{P_t} \triangleq \overline{P_R})-$ equivalence orbits, it follows

$$\dot{\alpha} = \dot{\bar{\alpha}} + \delta\dot{\alpha} = \overline{n_d} + \dot{\Omega}_s + \delta\dot{\alpha} = \overline{n_t} + \delta\dot{\alpha} \ \langle \sigma_i = +1 \ , \ \overline{n_t} < \dot{\Theta} \dot{\lambda} = \dot{\bar{\lambda}} + \delta\dot{\lambda} = \overline{n_d} + \dot{\Omega}_s - \dot{\Theta} + \delta\dot{\lambda} = \overline{n_t} - \dot{\Theta} + \delta\dot{\lambda} = \overline{n_R} + \delta\dot{\lambda} = -\overline{n_t} + \delta\dot{\lambda}, \tag{3.16}$$

therefore

$$\dot{\alpha} + \dot{\lambda} = \delta\dot{\alpha} + \delta\dot{\lambda}. \tag{3.17}$$

Neglecting the periodic parts, formula (3.9) yields

$$\dot{\bar{\alpha}} + \dot{\bar{\lambda}} = 2\overline{n_t} - \dot{\Theta} = 0 \ \langle \sigma_i = +1, \ \overline{n_R} = -\overline{n_t}. \tag{3.18}$$

After integration the characterizing relation for $(\overline{P_t} \triangleq \overline{P_R})-$ and $(P_t \triangleq P_R)-$ equivalence orbits will be obtained

$$\overline{\alpha} + \overline{\lambda} = const. \ =: \ \overline{Q} \ \langle \sigma_i = +1, \ \overline{n_R} = -\overline{n_t}. \tag{3.19}$$

that means, taking into account the secular orbit impacts only, the motion of the satellite in right ascension is direct whereas the motion in geographic longitude seems backward. The sum of these motions is constant with respect to the Earth's equator. The constant $\overline{Q}$ characterizes the equivalence orbit and should be called "equivalence factor". The periodic part in equation (3.17) has the integral

$$\delta Q := \int (\delta\dot{\alpha} + \delta\dot{\lambda}) \, dt. \tag{3.20}$$

therefore the general expression is

$$\alpha + \lambda = Q = \overline{Q} + \delta Q \langle \sigma_i = +1, \ \overline{n_R} = -\overline{n_t}. \tag{3.21}$$

This expression is highly remarkable. When coupling a tropical with a meridional motion only the periodic part will affect the sum of the right ascension and the geographic longitude. This periodic part will be composed of periodical physical impacts ("so-called periodic perturbations of a *Kepler*ian orbit"), the equation of the center in case of eccentric orbits and the reduction to the equator in case of inclined orbits. The secular parts however, which are combined in the mean motion, are completely eliminated.

2. The connection between right ascension and geographic longitude $\alpha = \lambda + \Theta_G$ is similarly valid for the ascending node

$$\Omega = \lambda_\Omega + \Theta_G. \tag{3.22}$$

Based on formula (3.21) the relationship follows for the (constant) equivalence factor $\overline{Q}$

$$\overline{Q} = 2\,\Omega - \Theta_G - \delta Q \ \langle \sigma_i = +1, \ \overline{n_R} = -\overline{n_t}. \tag{3.23}$$

Neglecting the periodic part in the right ascension of the ascending node $\delta\Omega = \Omega - \overline{\Omega}$ and in the factor δQ an important coherence between the right ascension of the ascending node and the mean equivalence factor $\overline{Q}$ can be found, which is valid at epoch t_0

$$\overline{Q} = \overline{Q}_0 = 2\overline{\Omega}_0 - \Theta_{G0} \ \langle \sigma_i = +1, \ \overline{n_R} = -\overline{n_t}. \tag{3.24}$$

that means: for $(\overline{P_t} \triangleq \overline{P_R})-$ as well as $(P_t \triangleq P_R)-$ equivalence orbits the mean equivalence factor $\overline{Q}$ can be used as an alternative to the mean orbital element $\overline{\Omega}_0$, when the sidereal time Θ_{G0} is known at epoch t_0.

3. The period of a $(\overline{P_t} \triangleq \overline{P_R})-$ as well as a $(P_t \triangleq P_R)-$ equivalence orbit is nearly 2 sidereal days as computed in Table 1. Based on this fact one can assume that such an orbit is highly stable with respect to the Earth's surface. This stability is an essential property of equivalence orbits coupling tropical and meridional motions.

There are two essential factors to characterize the orbit stability:

➢ The secular shift of the geographic longitude of the perigee based on the secular drift of the perigee longitude $\dot{\lambda}_{Ps}$

$$\Delta\lambda_P = \dot{\lambda}_{P_s} \, P_a \tag{3.25}$$

Table 3
Orbit characteristics of the loop $(P_t \triangleq P_R)-$ equivalence orbit $\overline{a_{QtR}} = 66929.579770$ km, $\bar{e}_0 = 0.0$, $\bar{i}_0 = 80°$, $\overline{\Omega}_0 = 120°$, $\overline{\omega}_0 = \overline{M}_{00} = 0°$ (the data are computed incl. periodic perturbations).

$(P_t \triangleq P_R)$	
$\overline{a_{QtR}} = 66929.579770$ km, $\bar{e}_0 = 0.8$, $\bar{i}_0 = 80°$, $\overline{\Omega}_0 = 120°$, $\overline{\omega}_0 = \overline{M}_{00} = 0°$	
$\overline{Q} = 86°.533884$	t_{01} : 2019 − 08 − 25/12:00:0.0
$\overline{P_K} = 172320.968888$ sec	
$\overline{P_H} = 172335.235914$ sec	$P_H = 172326.913672$ sec
$\overline{P_a} = 172326.319160$ sec	$P_a = 172326.319192$ sec
$\overline{P_d} = 172334.644838$ sec	$P_d = 172326.874228$ sec
$\overline{P_t} = 172338.049222$ sec	$P_t = 172328.181014$ sec
$\overline{P_R} = 172318.313935$ sec	$P_R = 172328.181014$ sec
$\overline{P_S} = 173284.386452$ sec	$P_S = 172662.142754$ sec
$\overline{P_S} = 173284.386451$ sec	$P_S = 172662.142754$ sec
$H_P = 7007.779354$ km	$H_A = 114095.106986$ km
$\overline{\Delta\lambda_P} = \dot{\lambda}_{Ps} \overline{P_a} = -720°.002352$	$\overline{\Delta\lambda_\Omega} = \dot{\lambda}_{\Omega s} \overline{P_d} = -720°.034118$
$\overline{\Delta\lambda_P} = \dot{\lambda}_{Ps} \overline{P_a} = -720°.002352$	$\overline{\Delta\lambda_\Omega} = \dot{\lambda}_{\Omega s} \overline{P_d} = -720°.001651$

characterizes the modification of the orbital shape over the Earth's surface, e.g. a tilting of the orbit.

➢ The secular shift of the nodal longitude based on the secular drift $\dot{\lambda}_{\Omega s}$ of the nodal longitude, and therefore on the whole orbit, is described by the term

$$\Delta\lambda_{\Omega} = \dot{\lambda}_{\Omega s}\, P_d. \tag{3.26}$$

3.2.3. Example of a $(P_t \triangleq P_R)-$ equivalence orbit

A $(P_t \triangleq P_R)-$ equivalence orbit with eccentricity $\overline{e}_0 = 0.8$ and inclination $\overline{i}_0 = 80°$ shall be selected.

The mean semimajor axis of a $(P_t \triangleq P_R)-$ equivalence orbit can be calculated using the condition functions (3.14) and (3.15). They use the true tropical period from (2.17) and the true meridional motion from (2.24). The mean semimajor axis will be $\overline{a_{QtR}}_{\text{sec}} = 66929.579760$ km respecting secular influences only, $\overline{a_{QtR}}_{per} = 66929.579770$ km including periodic influences.

The orbit characteristics are summarized in Table 3. It can be seen, that the ascending node will be shifted in westward direction by $\overline{\Delta\lambda_{\Omega}} = 0°.29$ during one year. The corresponding shift of the perigee longitude will be $\overline{\Delta\lambda_P} = 0°.42$. The anomalistic period is shorter than the draconitic period. Therefore after one or more periods the satellite will reach the perigee before crossing the node. This can be recognized in Fig. 4 which shows the groundtrack of this orbit for one period after epoch and again after one year. The meridional period is greater than the draconitic period. Therefore the satellite will reach the reference meridian after crossing the node. The corresponding point where the satellite intersects the reference meridian after one year is marked by "R". A three-dimensional presentation of the orbits is shown in Fig. 5 . The course of the right ascension and the corresponding geographic longitude as well as tjeir sum and the constant equivalence factor are compiled in (see Fig. 6.

The mean equivalence factor $\overline{Q}$ is calculated with the right ascension of the ascending node and the sidereal time $\Theta_G = 153°.466116$ at epoch time t_0. The equivalence factor is not influenced by the selected semi-major axis, as can be seen in formula (3.24). ◂

3.3. Coupling of anomalistic motion with meridional motion

Coupling the anomalistic with the meridional motion implicates a coupling of the true anomaly with a certain meridian. Especially the line of apsides will be connected with a meridian.

The $(\overline{P_a} \triangleq \overline{P_R})-$ equivalence orbit can be obtained by comparing the

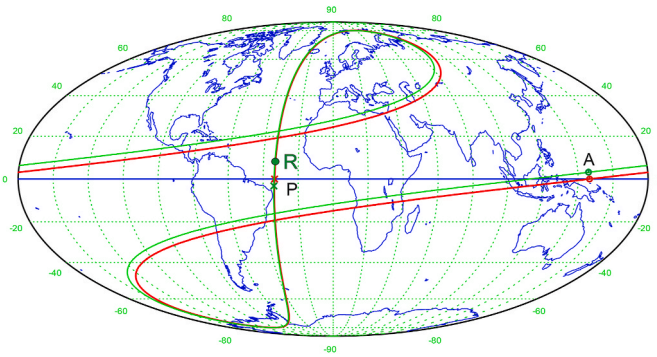

Fig. 4. Groundtrack of the elliptical $(P_t \triangleq P_R)-$ equivalence orbit with semi-major axis $\overline{a_{QtR}} = 66929.579770$ km, $\overline{e}_0 = 0.8$, $\overline{i}_0 = 80°$, $\overline{\Omega}_0 = 120°$, for one period (2 sidereal days) with apparent orbital loops. The red curve is drawn after the epoch t_0 : 2019 − 08 − 25/12:00:0.0, the overlapping green curve one year later. P marks the perigee, A the apogee. In point R the second orbit intersects the reference meridian. (For interpretation of the references to color in this figure legend, the reader is referred to the Web version of this article.)

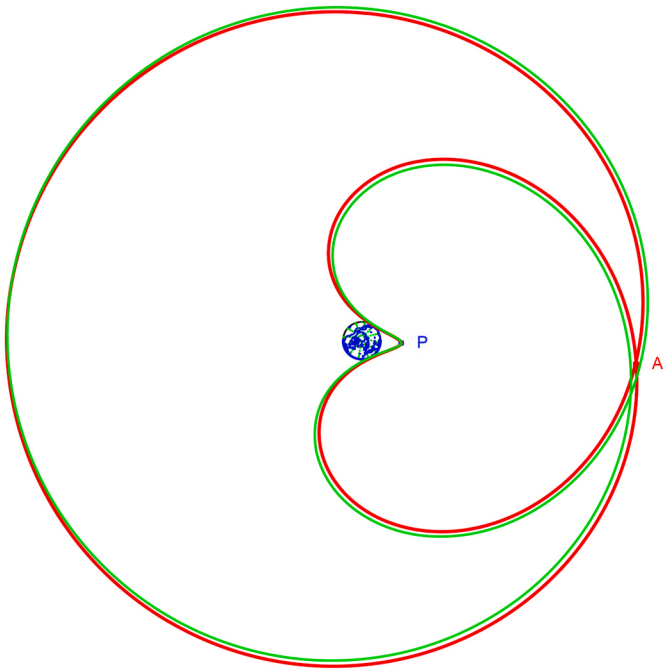

Fig. 5. True course of the $(P_t \triangleq P_R)-$ equivalence orbit $\overline{a_{QtR}} = 66929.579770$ km, $\overline{e}_0 = 0.8, \overline{i}_0 = 80°$, $\overline{\Omega}_0 = 220°$, $\overline{\omega}_0 = \overline{M}_{00} = 0°$ for 2 sidereal days, starting at epoch t_0 : 2019 − 08 − 25/12:00:0.0(red curve) and at t_2 : 2020 − 08 − 25/12:00:0.0(overlapping green curve). View direction: $\lambda = 340°$, $\varphi = 83°$. Perigee (P) and apogee (A) are marked. (For interpretation of the references to color in this figure legend, the reader is referred to the Web version of this article.)

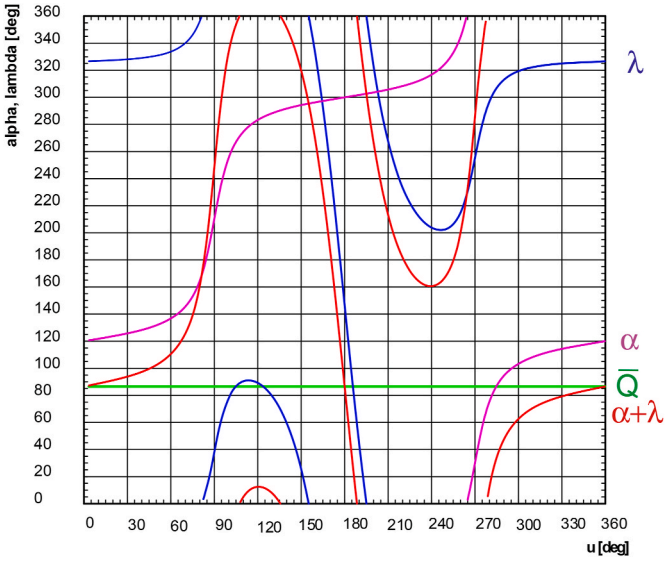

Fig. 6. Course of right ascension and geographic longitude and sum for one orbital period (2 sidereal days) of the $(\overline{P_t} \triangleq \overline{P_R})-$ equivalence orbit $\overline{a_{QtR}} = 66929.579770$ km, $\overline{e}_0 = 0.8$, $\overline{i}_0 = 80°$, $\overline{\Omega}_0 = 120°$, $\overline{\omega}_0 = \overline{M}_{00} = 0°$. Also in this case of true orbits the mean equivalence factor $\overline{Q}$ can be separated.

mean anomalistic mean motion (2.13) with the mean meridional mean motion (2.23)

$$\overline{n_R} = \overline{n_k} + (M_0)_s^{\cdot} + \dot{\omega}_s + \sigma_i\left(\dot{\Omega}_s - \dot{\Theta}\right) = \overline{n_a} + \dot{\omega}_s + \sigma_i\left(\dot{\Omega}_s - \dot{\Theta}\right). \tag{3.27}$$

Analogous to relation (3.8) we can derive the condition (compare Figs. 3–2 on page 12)

$$\overline{n_R} = -\overline{n_a} \Leftrightarrow \overline{P_a} = \overline{P_R} \ \langle \sigma_i = +1 \ . \tag{3.28}$$

The corresponding semimajor axis based on the mean *Keplerian* elements $(\bar{e}_0\ ,\ \bar{i}_0)$ can iteratively be computed using the condition equation

$$fct(\overline{a_{QaR}}) \equiv 2\,\overline{n_a} + \dot{\omega}_s + \dot{\Omega}_s - \dot{\Theta} = 0. \tag{3.29}$$

The theoretical value (3.12) can be used as a first approximation. The anomalistic mean motion and corresponding mean period follow from

$$\overline{n_a} = \frac{1}{2}\left(\dot{\Theta} - \dot{\omega}_s - \dot{\Omega}_s\right),\ \overline{P_a} = 2\pi\ /\overline{n_a}\ = \overline{P_R}. \tag{3.30}$$

In order to compute a $(P_a \triangleq P_R)-$ equivalence orbit based on the mean *Keplerian* elements $(\bar{e}_0\ ,\ \bar{i}_0\ ,\ \overline{\Omega}_0\ ,\ \overline{\omega}_0\ ,\ \overline{M_{00}})$ the true anomalistic period from (2.14) and the true meridional period from (2.24) can be used based on a preset semimajor axis

$$fct(P_a) \equiv \sin[v(t_0 + P_a) - v(t_0)] = 0, fct(P_R) \equiv \sin[\lambda(t_0 + P_R) - v(t_0)] = 0. \tag{3.31}$$

The mean semimajor axis will finally be obtained by the condition function

$$fct(\overline{a_{QaR}}) \equiv P_a - P_R = 0. \tag{3.32}$$

In practical application an accuracy e.g. of the order $\Delta t \approx 10^{-9}$ sec is required.

The period times of $(\overline{P_a} \triangleq \overline{P_R})-$ as well as $(P_a \triangleq P_R)-$ equivalence orbits differ with elements. This is a consequence of the condition equation (3.27) where the secular variations of the *Keplerian* elements Ω, ω are explicitly contained. See for example the numeric values compiled in Table 4.

3.4. Coupling of draconitic motion with meridional motion

Coupling of draconitic with meridional motion enforces the connection of a certain argument of latitude with a certain meridian. Especially the nodes of a satellite orbit can be fixed in geographic longitude when the position of a satellite at epoch is to be fixed with respect to the Earth surface.

A $(\overline{P_d} \triangleq \overline{P_R})-$ equivalence orbit can be obtained by comparison of the related mean motions (2.15) and (2.23)

$$\overline{n_R} = \overline{n_K} + (M_0)_s^{\cdot} + \dot{\omega}_s + \sigma_i\left(\dot{\Omega}_s - \dot{\Theta}\right) = \overline{n_d} + \sigma_i\left(\dot{\Omega}_s - \dot{\Theta}\right)\ . \tag{3.33}$$

Analogous to relation (3.8) we can also in this case obtain the condition (compare Fig. 3 on page 12)

$$\overline{n_R} = -\overline{n_d} \Leftrightarrow \overline{P_d} = \overline{P_R} \ \langle \sigma_i = +1. \tag{3.34}$$

The corresponding semimajor axis based on the mean *Keplerian* elements $(\bar{e}_0\ ,\ \bar{i}_0)$ can iteratively be computed using the condition equation

$$fct(\overline{a_{QdR}}) \equiv 2\,\overline{n_d} + \dot{\Omega}_s - \dot{\Theta} = 0 \ \langle \sigma_i = +1\ . \tag{3.35}$$

The theoretical value (3.12) can be used as a first approximation. The draconitic mean motion and corresponding period follow from

$$\overline{n_d} = \frac{1}{2}\left(\dot{\Theta} - \dot{\Omega}_s\right) = |\overline{n_R}|, \overline{P_d} = 2\pi\ /\overline{n_d}\ = \overline{P_R}. \tag{3.36}$$

In order to compute a $(P_d \triangleq P_R)-$ equivalence orbit based on the mean *Keplerian* elements $(\bar{e}_0\ ,\ \bar{i}_0\ ,\ \overline{\Omega}_0\ ,\ \overline{\omega}_0\ ,\ \overline{M_{00}})$ the true draconitic period from (2.16) and the true meridional period from (2.24) can be used based on a preset semimajor axis

$$fct(P_d) \equiv \sin[u(t_0 + P_d) + u(t_0)] = 0, fct(P_R) \equiv \sin[\lambda(t_0 + P_R) + \lambda(t_0)] = 0. \tag{3.37}$$

The mean semimajor axis $\overline{a_{QdR}}$ can finally be obtained applying the condition function

$$fct(\overline{a_{QdR}}) \equiv P_d - P_R = 0. \tag{3.38}$$

The theoretical value (3.12) can be used as first approximation for the iteration process (3.37)–(3.38). The period times of $(\overline{P_d} \triangleq \overline{P_R})-$ as well as $(P_d \triangleq P_R)-$ equivalence orbits differ with preset elements. This property is similar to the previous case, well-founded by the fact that condition equation (3.33) contains explicitly the secular variation of the right ascension of the ascending node $\dot{\Omega}_s$. See for example the numeric values in Table 5.

3.5. Coupling of hansen motion with meridional motion

Coupling a *Hansen*-with a meridional motion links a *Hansen* orbit angle with a special meridian. By this way a position within the orbital plane can be fixed above the meridian selected.

The $(\overline{P_H} \triangleq \overline{P_R})-$ equivalence orbit will be obtained by comparison of the related mean motions (2.8) and (2.23)

$$\overline{n_H} = \overline{n_K} + (M_0)_s^{\cdot} + \dot{\omega}_s + \dot{\Omega}_s \cos\bar{i}_0 = \overline{n_d} + \dot{\Omega}_s \cos\bar{i}_0, \overline{n_R} = \overline{n_d} + \sigma_i\left(\dot{\Omega}_s - \dot{\Theta}\right). \tag{3.39}$$

Analogous to relation (3.8) we can obtain the condition (compare Fig. 3: on page 11)

$$\overline{n_R} = -\overline{n_H} \Leftrightarrow \overline{P_H} = \overline{P_R} = 2\pi\ /|\overline{n_R}| \ \langle \sigma_i = +1. \tag{3.40}$$

the corresponding mean semimajor axis based on the mean *Keplerian* elements $(\bar{e}_0\ ,\ \bar{i}_0)$ can iteratively be computed using the condition equation

$$fct(\overline{a_{QHR}}) \equiv 2\,\overline{n_H} + \dot{\Omega}_s\left(1 - \cos\bar{i}_0\right) - \dot{\Theta} = 0. \tag{3.41}$$

The theoretical value (3.12) can be used as first approximation. The *Hansen* mean motion and corresponding mean period follow from

$$\overline{n_H} = \frac{1}{2}\left[\dot{\Theta} - \dot{\Omega}_s\left(1 - \cos\bar{i}_0\right)\right] = |\overline{n_R}|, \overline{P_H} = 2\pi\ /\overline{n_H}\ = \overline{P_R}. \tag{3.42}$$

In order to compute a $(P_H \triangleq P_R)-$ equivalence orbit based on the mean *Keplerian* elements $(\bar{e}_0\ ,\ \bar{i}_0\ ,\ \overline{\Omega}_0\ ,\ \overline{\omega}_0\ ,\ \overline{M_{00}})$ the true *Hansen* period from (2.12) and the true meridional period from (2.24) can be used based on a preset semimajor axis

$$fct(P_H) \equiv \sin[\zeta(t_0 + P_H) + \zeta(t_0)] = 0, fct(P_R) \equiv \sin[\lambda(t_0 + P_R) + \lambda(t_0)] = 0. \tag{3.43}$$

The mean semimajor axis $\overline{a_{QHR}}$can finally be obtained applying the condition function

$$fct(\overline{a_{QHR}}) \equiv P_H - P_R = 0. \tag{3.44}$$

Table 4
Example of the computation of semimajor axis and period of $(\overline{P_a} \triangleq \overline{P_R})-$ and $(P_a \triangleq P_R)-$ equivalence orbits with different inclinations, epoch 2019-10-16/00:00:0.00

$\bar{e}_0$	$\bar{i}_0$	$\overline{a_{QaR}}[\overline{P_a} \triangleq \overline{P_R}]$	$\overline{P_a} = \overline{P_R}$	$\overline{a_{QaR}}[P_a \triangleq P_R]$	$P_{a,\mathrm{sec}} = P_{R,\mathrm{sec}}$
0.3	0°	66932.602551 km	172329.715502 s	66932.602551 km	172329.715503 s
	30°	66932.123196 km	172328.962002 s	66932.0550010 km	172328.679351 s
	60°	66931.203475 km	172327.605592 s	66931.178646 km	172327.509704 s
	85°	66930.851119 km	172327.309226 s	66931.025570 km	172327.982958 s

Table 5
Example of the computation of semimajor axis and period of $(\overline{P_d} \triangleq \overline{P_R})-$ and $(P_d \triangleq P_R)-$ equivalence orbits with different inclinations, epoch 2019-10-16/00:00:0.00

$\overline{e}_0$	$\overline{i}_0$	$\overline{a_{QdR}}[\overline{P_d} = \overline{P_R}]$	$\overline{P_d} = \overline{P_R}$	$\overline{a_{QdR}}[P_d = P_R]$	$P_{d,\mathrm{sec}} = P_{R,\mathrm{sec}}$
0.3	0°	66933.397154 km	172326.646639 s	66932.602555 km	172329.715489 s
	30°	66932.669484 km	172326.852200 s	66932.138114 km	172326.852195 s
	60°	66931.253132 km	172327.413816 s	66931.204832 km	172327.413815 s
	85°	66930.660010 km	172328.047282 s	66930.845896 km	172328.047282 s

Table 6
Examples of the computation of semimajor axis and period of $(\overline{P_H} \triangleq \overline{P_R})-$ and $(P_H \triangleq P_R)-$ equivalence orbits with different inclinations, $\overline{\Omega}_0 = \overline{\omega}_0 = \overline{M_{00}} = 0°$, epoch 2019-10-16/00:00:0.00

$\overline{e}_0$	$\overline{i}_0$	$\overline{a_{QHR}}[\overline{P_H} \triangleq \overline{P_R}]$	$\overline{P_H} = \overline{P_R}$	$\overline{a_{QHR}}[P_H \triangleq P_R]$	$P_{H,\mathrm{sec}} = P_{R,\mathrm{sec}}$
0.3	0°	66932.999861 km	172328.181014 s	66932.591714 km	172331.249912 s
	30°	66932.371510 km	172328.002975s	66932.090058 km	172327.848802 s
	60°	66931.153806 km	172327.797404 s	66931.152456 km	172327.605610 s
	85°	66930.656992 km	172328.058937 s	66930.843059 km	172328.048298 s

Again, the theoretical value (3.12) can be used as a first approximation. Table 6 shows also in the case of *Hansen* motions each set of preset orbital elements will cause different orbital periods.

3.6. Coupling of Sun-synodic motion with meridional motion

Coupling of Sun-synodic and meridional motion links a fixed solar time in subsatellite point with a fixed meridian when overflown in the same apparent flight direction: $(\overline{P_S} \triangleq \overline{P_R})-$ equivalence means same mean solar time, $(P_S \triangleq P_R)-$ equivalence means same true solar time.

3.6.1. Basic characteristics

A $(\overline{P_S} \triangleq \overline{P_R})-$ equivalence orbit can be obtained by comparison of the related mean motions (2.23) and (2.33)

$$\left.\begin{aligned} \overline{n_S} &= \overline{n_K} + (M_0)_s^{\cdot} + \dot{\omega}_s + \sigma_i \left(\dot{\Omega}_s - n_\mathrm{A}\right) = \overline{n_t} - \sigma_i\, n_\mathrm{A} = \overline{n_t} - n_\mathrm{A} \\ \overline{n_R} &= \overline{n_K} + (M_0)_s^{\cdot} + \dot{\omega}_s + \sigma_i \left(\dot{\Omega}_s - \dot{\Theta}\right) = \overline{n_t} - \sigma_i\, \dot{\Theta} = \overline{n_t} - \Theta \end{aligned}\right\} \sigma_i = +1 \tag{3.45}$$

Analogous to relations (3.7) and (3.8) we get also in this case the condition (compare Fig. 3: on page 12)

$$|\overline{n_R}| = \overline{n_S}, \overline{n_R} = -\overline{n_S} \Rightarrow \overline{n_R} + \overline{n_S} = 0 \,\langle \overline{P_S} = \overline{P_R} \tag{3.46}$$

Using the relation (2.26) between the tropical rotational rate of the Earth and the mean motion of the fictitious mean Sun n_A, the general relations (3.45) and respecting condition (3.46) yield

$$\begin{aligned} &\overline{n_R} + \overline{n_S} = 2\,\overline{n_t} - (\dot{\Theta} + n_\mathrm{A}) = 2\,\overline{n_t} - (1 + 2\,n_\mathrm{A}) = 0 \\ &\Leftrightarrow 2\,(\overline{n_t} - n_\mathrm{A}) - 2\pi/86400\ s = 2\,\overline{n_S} - 2\pi/86400\ s = 0\,. \end{aligned} \tag{3.47}$$

Therefore the mean Sun-related mean motion of a (theoretical) $(\overline{P_S} \triangleq \overline{P_R})-$ equivalence orbit has the value

$$\overline{n_{SQR}} = \pi \,/\, 86400\ \mathrm{s} = 3.63610261 \times 10^{-5}\ [1/\mathrm{s}]. \tag{3.48}$$

Correspondingly the period of such an orbit is exactly 2 solar days

$$\overline{P_S} = \overline{P_R} = 2\pi \,/\, \overline{n_{SQ}} = 172800\ \mathrm{s}\ \langle \overline{P_S} = \overline{P_R}. \tag{3.49}$$

The mean semimajor axis of the *Kepler*ian $(\overline{P_S} \triangleq \overline{P_R})-$ equivalence orbit (as computed with *Kepler*'s third law) is

$$\overline{a_{QSR}}_K = \sqrt[3]{\mu\, \overline{P_S}_K^2 \,/\, (4\pi^2)} = 67053.559276\ \mathrm{km}. \tag{3.50}$$

For a preset eccentricity $\overline{e}_0$and inclination $\overline{i}_0$the mean semimajor axis of a $(\overline{P_S} \triangleq \overline{P_R})-$ equivalence orbit can iteratively be computed with the help of the condition equation

$$fct(\overline{a_{QSR}}) \equiv 2\pi \,\Big/\, \overline{n_S} - 2\pi \,/\, \overline{n_R} = \overline{P_S} - \overline{P_R} = 0 \tag{3.51}$$

with (3.50) or (3.12) as a first approximation. The result is valid for the epoch $t_0$of the preset mean *Kepler*ian parameters.

Using the true solar angle (2.28) $\tau = \alpha - \alpha_\mathrm{A}$as the orbit angle of the Sun-synodic motion, the geographic longitude for the meridional motion, the preset *Kepler*ian orbital parameters $(\overline{e}_0\ ,\ \overline{i}_0\ ,\ \overline{\Omega}_0\ ,\ \overline{\omega}_0\ ,\ \overline{M_{00}})$ and a suitable semimajor axis, the true periods can be calculated from

$$fct(P_S) \equiv \sin[\tau(t_0 + P_S) - \tau(t_0)] = 0, fct(P_R) \equiv \sin[\lambda(t_0 + P_S) - \lambda(t_0)] = 0. \tag{3.52}$$

The correct semimajor axis of the selected $(P_S \triangleq P_R)-$ equivalence orbit can finally be obtained from

$$fct(\overline{a_{QSR}}) \equiv P_S - P_R = 0. \tag{3.53}$$

The whole process has to be treated iteratively, again based on (3.50) or (3.12) as a first approximation.

3.6.2. Further general characteristics

1. Further investigations require the mean solar angle with respect to the fictitious mean Sun

$$\overline{\tau} = \overline{\alpha} - \alpha_{\overline{\mathrm{A}}} \text{ with } \alpha_{\overline{\mathrm{A}}} = \alpha_{\overline{\mathrm{A}}0} + n_\mathrm{A}\,(t - t_0) + \cdots \tag{3.54}$$

and its variations

$$\dot{\tau} = \dot{\alpha} - \dot{\alpha}_\mathrm{A}, \dot{\overline{\tau}} = \dot{\overline{\alpha}} - \dot{\alpha}_{\overline{\mathrm{A}}} = \dot{\overline{\alpha}} - n_\mathrm{A}. \tag{3.55}$$

Similarly to relationship (3.16) using (2.23) and (2.19) with periodic parts $(\delta\dot{\tau},\ \delta\dot{\lambda})$, we can obtain

$$\dot{\tau} = \dot{\overline{\tau}} + \delta\dot{\tau} = \dot{\overline{\alpha}} - n_0 + \delta\dot{\tau} = \overline{n_t} - n_0 + \delta\dot{\tau} = \overline{n_S} + \delta\dot{\tau}\dot{\lambda} = \dot{\overline{\lambda}} + \delta\dot{\lambda} = \overline{n_t} - \dot{\Theta} + \delta\dot{\lambda} = \overline{n_R} + \delta\dot{\lambda} = -\overline{n_S} + \delta\dot{\lambda}\rangle\ \sigma_i = +1\ ,\ \overline{n_t} < \dot{\Theta} \tag{3.56}$$

Table 7
Computation of the mean semimajor axis of some $(\overline{P_S} \triangleq \overline{P_R})$ – equivalence and $(P_S \triangleq P_R)$– equivalence orbits, $\overline{\Omega} = \overline{\omega} = \overline{M_0} = 0$, epoch: 2019-10-16/00:00:0.00, basic parameters: $R_E = 6378.1366$ km, $\mu_E = 398600.4418\ \mathrm{km}^3/\mathrm{s}^2$, $\dot{\Theta} = 0.72921158573340 \times 10^{-4}$ /s.

$\overline{e}_0$	$\overline{i}_0$	$\overline{a_{QSR}}[\overline{P_S} \triangleq \overline{P_R}]$	$\overline{P_S} = \overline{P_R}$	$\overline{a_{QSR}}[P_S \triangleq P_R]$	$P_{S,\mathrm{sec}} = P_{R,\mathrm{sec}}$
0.0	0°	66811.207620 km	172800.000 s	66817.445012 km	172775.674 s
	30°	66810.636714 km	172800.000 s	66781.238046 km	172775.674 s
	60°	66809.559569 km	172800.000 s	66586.794182 km	172775.674 s
	85°	66809.192544 km	172800.000 s	64611.874565 km	172775.674 s
0.3	0°	66811.444649 km	172800.000 s	66929.446777 km	172775.674 s
	30°	66810.768974 km	172800.000 s	66910.560004 km	172775.674 s
	60°	66809.495727 km	172800.000 s	66809.562272 km	172775.674 s
	85°	66809.065849 km	172800.000 s	65755.532145 km	172775.674 s
0.6	0°	66812.786298 km	172800.000 s	67002.477654 km	172775.674 s
	30°	66811.513056 km	172800.000 s	66994.629629 km	172775.674 s
	60°	66809.124653 km	172800.000 s	66954.179216 km	172775.674 s
	85°	66808.345692 km	172800.000 s	66532.937085 km	172775.674 s
0.9	0°	66836.147849 km	172800.000 s	67050.298487 km	172775.674 s
	30°	66824.163694 km	172800.000 s	67046.233384 km	172775.674 s
	60°	66802.037123 km	172800.000 s	67035.263925 km	172775.674 s
	85°	66795.629900 km	172800.000 s	66983.153543 km	172775.674 s

therefore

$$\dot{\tau} + \dot{\lambda} = \dot{\overline{\tau}} + \dot{\overline{\lambda}} + \delta\dot{\tau} + \delta\dot{\lambda} = \delta\dot{\tau} + \delta\dot{\lambda}. \tag{3.57}$$

Neglecting the periodic parts it remains

$$\dot{\overline{\tau}} + \dot{\overline{\lambda}} = 0 \ \langle \sigma_i = +1,\ \overline{n_R} = -\overline{n_S}\ . \tag{3.58}$$

Integration leads to the necessary and sufficient characterizing relationship for $(\overline{P_S} \triangleq \overline{P_R})$ – equivalence orbits

$$\overline{\tau} + \overline{\lambda} = const. \quad =: \ \overline{Q_S}\ \langle \sigma_i = +1,\ \overline{n_R} = -\overline{n_S}\ . \tag{3.59}$$

The satellite is moving eastward with respect to the fictitious mean Sun whereas it seems to move westward with decreasing geographic longitude. The sum of the mean part of these two angles is constant. The corresponding constant equivalence factor $\overline{Q_S}$ is characterizing the $(\overline{P_S} \triangleq \overline{P_R})$ – equivalence orbit.

Integration of the differential equation (3.57) leads with the periodic part to the general expression

$$\tau + \lambda = Q_S = \overline{Q_S} + \delta Q_S, \delta Q_S := \int (\delta\dot{\tau} + \delta\dot{\lambda})\, dt\ \langle \sigma_i = +1,\ \overline{n_R} = -\overline{n_S}. \tag{3.60}$$

It should be noted that in case of a $(P_S \triangleq P_R)$ – equivalence orbit the sum of solar angle and geographic longitude only undergo periodic variations. These variations are composed by the periodic orbital impacts ("periodic perturbations"), the equation of the center in case of elliptic motion and the reduction to the equator in case of inclined orbits. However the secular effects summarized in the mean motion are eliminated.

1. The mean solar angle of the ascending node at epoch is known by

$$\overline{\tau_{\Omega 0}} = \overline{\Omega}_0 - \alpha_{\overline{\gamma}_{00}} \tag{3.61}$$

whereas the geographic longitude of the ascending node using formula (3.22) is given by

$$\overline{\lambda_{\Omega 0}} = \overline{\Omega}_0 - \Theta_{G0} \tag{3.62}$$

The constant mean equivalence factor of a $(\overline{P_S} \triangleq \overline{P_R})$ – equivalence orbit will get, following formula (3.59), the relationship

$$\overline{Q_{S0}} = 2\overline{\Omega}_0 - \alpha_{\overline{\gamma}_{00}} - \Theta_{G0}\ \langle \sigma_i = +1,\ \overline{n_R} = -\overline{n_S}. \tag{3.63}$$

Therefore analog to the case (3.24) the mean equivalence factor $\overline{Q_{S0}}$ of a $(\overline{P_S} \triangleq \overline{P_R})$ – equivalence orbit can be taken as an orbital parameter instead of the right ascension of the ascending node $\overline{\Omega}_0$.

Table 7 shows some examples of the computation of the mean semimajor axis of Sun-related equivalence orbits with respect to meridional motion. The left columns for $(\overline{P_S} \triangleq \overline{P_R})$ – equivalence orbits are calculated using the condition function (3.51). They depend only on the epoch elements eccentricity and inclination $(\overline{e}_0, \overline{i}_0)$. It is remarkable that all periods for $(\overline{P_S} \triangleq \overline{P_R})$ – equivalence as well as for $(P_S \triangleq P_R)$ – equivalence are identical as necessary for this kind of equivalence orbits: refer to relationship (3.49). The value of the mean period matches with the theoretical value (3.49) within the accuracy 10^{-3} sec as consequence of the selected astronomical parameters. The values of the semimajor axis will slightly change with any other epoch.

3.7. Coupling of moon-synodic motion with meridional motion

Along with Sun-synodic motions, Moon-synodic motion can be investigated with equivalence to meridional motion.

Table 8
Comparative values of different equivalence orbits.

Table 1 $\left(\overline{e}_0 = 0.3,\ \overline{i}_0 = 85°\right)$	$\overline{a_{QtR}} = 66930.472364$ km	$P_t = P_R = 172328.181014$ s
Table 4 $\left(\overline{e}_0 = 0.3,\ \overline{i}_0 = 85°\right)$	$\overline{a_{QaR}} = 66931.025570$ km	$P_a = P_R = 172327.982958$ s
Table 5 $\left(\overline{e}_0 = 0.3,\ \overline{i}_0 = 85°\right)$	$\overline{a_{QdR}} = 66930.845896$ km	$P_d = P_R = 172328.047282$ s
Table 6 $\left(\overline{e}_0 = 0.3,\ \overline{i}_0 = 85°\right)$	$\overline{a_{QHR}} = 66930.843059$ km	$P_H = P_R = 172328.048298$ s

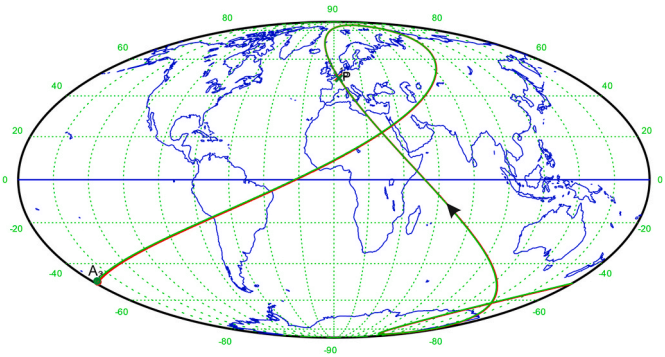

Fig. 7. Subsatellite track of the $(P_H \triangleq P_a \triangleq P_d \triangleq P_t \triangleq P_R)-$ equivalence orbit with *Kepler*ian orbital parameter $\bar{e}_0 = 0.3$, $\bar{i}_0 = 85°$, $\overline{\Omega}_0 = 145°$, $\overline{\omega}_0 = 50°$, $\overline{M_{00}} = 0°$. The computed semimajor axis is $\overline{a_{QR}} = 66930.845889$ km. The orbit is drawn, starting at epoch t_0 : $2019-08-19/12{:}00{:}0.0$in red color and one year later at epoch $t_{02}: 2020-08-19/12{:}00{:}0.00$ in overlapping green color. In both cases the orbit is presented for one period (2 sidereal days) showing a nearly perfect stability of this orbit over long time intervals. (For interpretation of the references to color in this figure legend, the reader is referred to the Web version of this article.)

Table 9
Orbit characteristics of a multiple equivalence orbit based on equivalent true *Hansen*, anomalistic, draconitic, tropical and meridional motion.

$(P_H \triangleq P_a \triangleq P_d \triangleq P_t \triangleq P_R)$	
$\overline{a_{QSR}} =$ 66930.845896 km, $\bar{e}_0 = 0.3$, $\bar{i}_0 = 85°$, $\overline{\Omega}_0 = 145°$, $\overline{\omega}_0 = 50°$, $\overline{M_{00}} = 0°$	
$\overline{Q} = 142°.447768$	t_0 : $2019-08-19/12{:}00{:}0.0$
$\overline{P_H} = 172328.788488$ sec	$P_H = 172328.059254$ sec
$\overline{P_a} = 172327.289055$ sec	$P_a = 172327.289479$ sec
$\overline{P_d} = 172328.765176$ sec	$P_d = 172328.047282$ sec
$\overline{P_t} = 172329.032639$ sec	$P_t = 172328.705691$ sec
$\overline{P_R} = 172327.329397$ sec	$P_R = 172328.047282$ sec
$\overline{P_S} = 173275.270575$ sec	$P_S = 174180.054104$ sec
$\overline{P_L} = 185900.250963$ sec	$P_L = 192041.352703$ sec
$H_P = 40473.455527$ km	$H_A = 80631.963065$ km
$\overline{\Delta\lambda_P} = \dot{\lambda}_P \overline{P_a} = -719°.997476$	$\overline{\Delta\lambda_\Omega} = \dot{\lambda}_{\Omega s} \overline{P_d} = -720°.002999$
$\Delta\lambda_P = \dot{\lambda}_P P_a = -719°.997478$	$\Delta\lambda_\Omega = \dot{\lambda}_{\Omega s} P_d = -720°.000000$

3.8. Multiple coupling equivalence orbits

In the previous sections the coupling between two kinds of satellite motion was investigated where one of these motions was always the meridional motion. In all cases, the choice of the *Kepler*ian parameters $(\bar{e}_0, \bar{i}_0, \overline{\omega}_0, \overline{M_{00}})$ greatly influences the value of the semimajor axis of such an equivalence orbit. However Fig. 2, Table 4, Table 5, Table 6 show the influence on to the semimajor axis as well as on the periods in the case of *Hansen*, anomalistic, draconitic motion and the tropical motion. Therefore one may assume that by a suitable selection of the *Kepler*ian parameters an appropriate *Hansen*, anomalistic, draconitic orbit can be selected, whose semimajor axis and period matches the tropical or the Sun-synodic motion. Such multiple equivalence orbits could be of great importance when looking for a longterm stable satellite orbit with respect to the Earth's surface.

EXAMPLE: The equivalence orbit $\left(\bar{e}_0 = 0.3,\ \bar{i}_0 = 85°\right)$includes the comparative values found summarized in Table 8.

Fig. 7 shows the $(P_t \triangleq P_a \triangleq P_d \triangleq P_H \triangleq P_R)-$ equivalence orbit with preset *Kepler*ian parameters $\left(\bar{e}_0 = 0.3,\ \bar{i}_0 = 85°,\ \overline{\Omega}_0 = 145°,\ \overline{\omega}_0 = 50°,\ \overline{M_{00}} = 0°\right)$ and computed semimajor axis $\overline{a_{QdR}} = 66930.845896$ kmfor one period (2 sidereal days) at two different dates spread over one year. It can be seen that not only the perigees (P) and apogees (A) and the nodes are coupled with the geographical net and therefore with the tropical equatorial coordinate system, but also the whole orbit. The characterizing properties of this orbit are compiled in Table 9. They show some different interesting properties of orbits with multiple equivalences. For instance, the nodal shift is negligible. The shift of the perigee towards east is less than 0°.5 per year. ◂

The example proves the existence of interesting satellite orbits with multiple equivalences. These special features are related to the coupling with meridional motions. This causes stability with respect to the Earth's surface. Equivalence orbits with reference to the Sun will induce stability in solar time. However looking at the relevant tables there is less similarity of the values with the Sun motion. Therefore time stability with multiple equivalences is hard to find. In reality, small deviations to the results presented in this example are to be expected due to physical influences from gravitational effects from Moon and Sun as well as other higher- order "perturbations" on the *Kepler*ian motion. The results presented might be improved using optimization methods. The principal properties however will certainly not be changed.

4. Equivalence orbits related to sun-synodic motion

Similarly to the coupling of satellite motions with meridional motions, equivalence orbits coupled to the Sun can be found and investigated with similar methods.

Consider the $(\overline{P_d} \triangleq \overline{P_S})-$ equivalence orbit as an example. The relevant orbits are the well-known Sun-synchronous orbits, which are only defined for retrograde orbits. The theory of equivalence orbits however can extend the investigations to $(P_d \triangleq P_S)-$ equivalence orbits, as well as any other coupled motions. In all these cases, an intersection between the different motions with the Sun-synodic motion is clearly defined. Therefore a unique solution for the semimajor axis can be found.

In a similar way equivalence orbits related to Moon-synodic motion can be handled.

5. Near parallel equivalence satellite orbits

A third group of equivalence orbits can be found by coupling *Hansen*, anomalistic, draconitic and tropical motions. From Figs. 3–2 it can be concluded that there is no well-defined intersection between the curves of these periods. The curves are more or less parallel, with small varying distances. Therefore a unique solution in searching for an equivalence orbit cannot be expected. However, also in this case a solution with lower accuracy of the order $\Delta t = \pm 0.01$ sec can be constructed in some interesting examples, as demonstrated in the following.

5.1. Example of coupling anomalistic and draconitic motion

A coupling of a satellite motion in relation to the line of apsides and the line of nodes will be achieved by the equivalence between the anomalistic and the draconitic satellite motion.

In order to construct a $(\overline{P_a} \triangleq \overline{P_d})-$ equivalence orbit the mean anomalistic mean motion (2.13) can be compared with the mean draconitic mean motion (2.15)

$$\overline{n_d} = \overline{n_a} + \dot{\omega}_s = \overline{n_a} \Rightarrow \dot{\omega}_s = 0 \Leftrightarrow \overline{P_d} = 2\pi \ / \overline{n_d} = 2\pi \ / \overline{n_a} = \overline{P_a}. \tag{5.1}$$

In first order the secular drift of the argument of perigee [1].

$$\dot{\omega}_{Gs} = -3\ \overline{n_{K0}}\ J_2\ R_E^2\ \left(1 - 5\cos^{2-}_{i_0} 0\right)\ /\ \left(4\,\overline{p}_0^2\right) + \ldots \tag{5.2}$$

vanishes for the critical inclination

$$1 - 5\cos^2 i_{krit} = 0 \Rightarrow \overline{i_{krit1}} = 63°.43495,\ \ \overline{i_{krit2}} = 116°.56505\,. \tag{5.3}$$

The well-known *Molnija* orbits $\left(\overline{a_{Qad}} = 26554.2276\ \text{km},\ \bar{e}_0 = 0.7222,\ \bar{i}_0 = 63°.434950\right)$use the critical inclination in order to

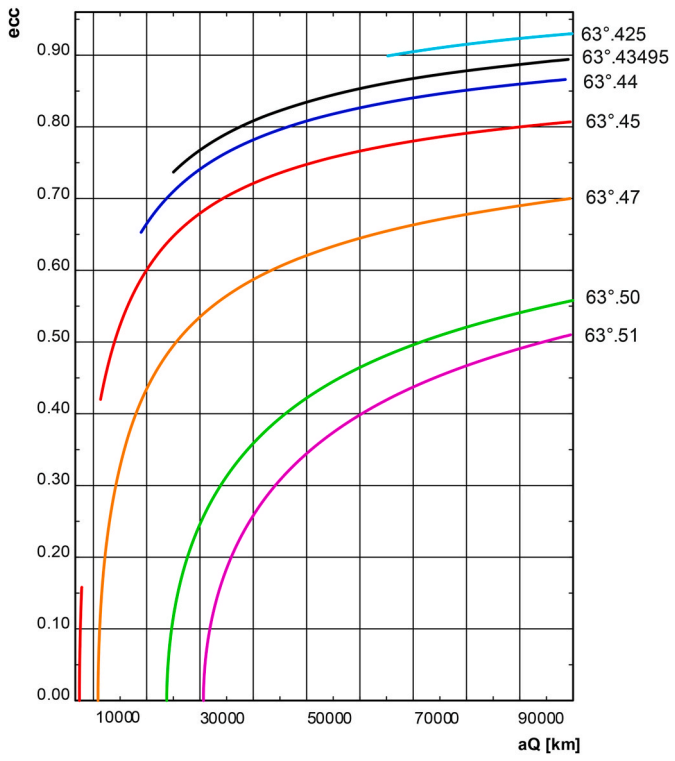

Fig. 8. Relation between eccentricity and semimajor axis for $(\overline{P_a} \triangleq \overline{P_d})-$ near equivalence orbits parametrized for inclinations near the critical inclination, computed with $\Delta a = 1$ km, $|\Delta t| < 0.01$ sec and minimum perigee height $H_P = 200$ km.

fix the line of apsides inertially.

However formula (5.2) will not exactly fulfill condition (5.1) so that some solutions of the condition function

$$fct(\overline{a}_0) \equiv \overline{P_a} - \overline{P_d} = 0 \tag{5.4}$$

in the vicinity of the critical inclination are possible. A survey of possible $(\overline{P_a} \triangleq \overline{P_d})-$ near equivalence orbits will be presented in Fig. 8. It shows the multiplicity of possible orbits which are given as curves *eccentricity* versus the *semimajor axis* and parametrized for some inclinations near the critical inclination. The computation for the plot uses the step size $\Delta a = 1$ km, $\Delta e = 0.001$, the accuracy limit $|\Delta P| < 0.01$ sec and shows orbits only with perigee height 200 km and above.

A possible orbit can be constructed by selection of an inclination not far away from the critical inclination. Any eccentricity might be chosen.

The iteration process to find a suitable solution can start with the semimajor axis $\overline{a_{Qad}}^{(0)} = R_E + 200$ km. The semimajor axis selected will be increased with a preset step size Δa. Then the difference (5.4) will be investigated at each step. Reaching the accuracy limit $\Delta t_{\text{limit}} = \left|\overline{P_a} - \overline{P_d}\right|$ the calculation stops with the semimajor axis obtained. In this way a lot of near equivalence orbits could be found. They are functions of the step size $\Delta a$and the accuracy Δt. Practical application shows that meaningful results will be obtained for required accuracy limits $|\Delta t_{\text{limit}}| < 0.01$ seconly.

$(P_a \triangleq P_d)-$ equivalence orbits will be calculated with condition equations (2.14) and (2).16)

$$fct(P_a) \equiv \sin[v(t_0 + P_a) - v(t_0)] = 0, fct(P_d) \equiv \sin[u(t_0 + P_d) - u(t_0)] = 0 \tag{5.5}$$

from

$$fct\left(\overline{a_{Qad_0}}\right) \equiv P_a - P_d = 0. \tag{5.6}$$

Again the semimajor $\overline{a_{Qad}}^{(0)} = 6578$ kmcan be used as starting value. The computation is stable.

NUMERICAL EXAMPLE: Let be preset the eccentricity $\overline{e}_0 = 0.7222$ and the inclination $\overline{i}_0 = 63°.45$. A $(\overline{P_a} \triangleq \overline{P_d})-$ equivalence orbit should be computed. The iteration (5.4) with step size $\Delta a = 1$ kmand accuracy limit $\Delta[fct(\overline{a}_0)] = 10^{-2}$ leads to the semimajor axis $\overline{a_{Qad}} = 40301.0$ kmwith periods $\overline{P_a} = 80518.460567$ secand $\overline{P_d} = 80518.460567$ sec.

Using the time limit 0.1 s would lead to a useless orbit with negative perigee height. This shows the extreme sensitivity in selection of a suitable near parallel equivalence orbit. The drift of the nodal longitude as shown in Table 10 is essentially a consequence of the Earth rotation. As to be expected from condition (5.7) the secular drift of the argument of perigee is extremely small $\dot{\omega}_s = -0.969144986 \times 10^{-11}$ rad/sec .◀

Table 10
Orbit characteristics of a $(\overline{P_a} \triangleq \overline{P_d})-$ equivalence orbit.

$(\overline{P_a} \triangleq \overline{P_d})$	
$\overline{a_{Qad}} = 40301.000$ km, $\overline{e}_0 = 0.7222$, $\overline{i}_0 = 63°.45$, $\overline{\Omega}_0 = \overline{\omega}_0 = \overline{M}_{00} = 0°$	
t_0 : 2029 − 08 − 19/12 : 00 : 0.0	
$\overline{P_K} = 80516.467775$ sec	$P_H = 80516.467775$ sec
$\overline{P_a} = 80518.460567$ sec	$P_a = 80518.460567$ sec
$\overline{P_d} = 80518.460567$ sec	$P_d = 80518.460567$ sec
$\overline{P_t} = 80524.855117$ sec	$P_t = 80524.855117$ sec
$\overline{P_R} = 1230369.149390$ sec	$P_R = 1249428.513102$ sec
$\overline{P_S} = 80730.858733$ sec	$P_S = 80590.858733$ sec
$\overline{P_L} = 83368.750768$ sec	$P_L = 83368.750768$ sec
$H_P = 4817.481$ km	$H_A = 63028.245$ km
$\overline{\Delta\lambda_P} = \dot{\lambda}_{Ps}\,\overline{P_a} = -336°.440670$	$\overline{\Delta\lambda_\Omega} = \dot{\lambda}_{\Omega s}\,\overline{P_d} = -336°.440692$
$\Delta\lambda_P = \dot{\lambda}_{Ps}\,P_a = -336°.440670$	$\Delta\lambda_\Omega = \dot{\lambda}_{\Omega s}\,P_d = -336°.440692$

6. Compendium of some characteristics of equivalence orbits

(I) General properties
- (1) Equivalence orbits are satellite orbits where two or more kinds of satellite relative motions are coupled.
- (2) In the frame of satellite orbit analysis the condition for equivalence can be used to select one orbital element, when all other elements are preset.
- (3) Multiple equivalence orbits can be used to select two or more orbital elements.
- (4) With respect to celestial mechanics background equivalence orbits can be interpreted as a kind of resonance effect between different motions.
- (5) Divers equivalence orbits can show a totally different orbit behavior.

(II) Equivalence orbits related to meridional motion
- (1) Suchlike orbits are always direct orbits.
- (2) Equivalence orbits with coupling of any satellite motion with the meridional motion have a mean semimajor axis in the range of 66931.447 km.
- (3) Meridian related Equivalence orbits usually show a longterm very stable orbit behavior with respect to the Earth's surface.
- (4) Equivalence orbits with coupling of the tropical with the meridional motion show the following remarkable characteristics:
  - ➢ The period is exactly 2 sidereal days ($47^h52^m08^s.1811$).
  - ➢ The sum of right ascension and geographic longitude of a satellite position shows periodic variations only. The sum of the mean values is constant (equivalence factor).

- ➢ The equivalence factor is coupled with the right ascension of the ascending node as an orbital element via the sidereal time at epoch.
- ➢ The mathematical formulation of the equivalence between tropical and meridional motion can be used as verification of the consistency of the basic physical parameters.

(III) Equivalence orbits related to Sun-synodic motion.

(1) Equivalence orbits by coupling of Sun-synodic and meridional motion show the following characteristics:
- ➢ The period of the mean motions is exactly 2 solar days (48 h).
- ➢ The period of the true motions is nearly 2 solar days as a consequence of the difference between fictive mean and true Sun, but always identical for different orbital elements and related to the same epoch.
- ➢ The sum of solar angle of the fictitious mean Sun and the geographic longitude of the satellite's position shows periodic variations only. The sum of the corresponding values is constant (equivalence factor for Sun-synodic motions).
- ➢ The equivalence factor for Sun-synodic motions can be assumed as an orbital element due to its relation to the right ascension of the ascending node via the sidereal time at epoch.
- ➢ The mathematical formulation of the equivalence between Sun-synodic and meridional motion can be used as verification of the consistency of the basic physical parameters.

(2) Sun-synchronous orbits can be interpreted as equivalence orbits formed by coupling of mean Sun-synodic with mean draconitic motion. They are always retrograde orbits.

(IV) Near equivalence orbits

(1) If a clearly defined intersection between two different satellite motions is not possible, near equivalence orbits can nevertheless be defined. It is possible to search for those orbits based on a restricted accuracy requirement and by means of a suitable search strategy. Usually the semimajor axis will be found with a preset step size. Dependent from these boundary conditions more than one near equivalence orbits can be found fulfilling the equivalence conditions.

(2) As an example the near coupling of a mean anomalistic and a mean draconitic motion is considered:
- ➢ The orbital inclination of this kind of equivalence orbits has the value in the range of 63°.44 or 116°.56. All eccentricities $e \in [0°,90°)$ are possible. The selection of the semimajor axis depends from eccentricity and inclination.
- ➢ Molnija and Tundra orbits can be considered as near equivalence orbits by coupling of mean anomalistic and mean draconitic motion.

7. Final remark

The employment with equivalence orbits is a special point of view in order to investigate satellite orbits. Not only unknown orbit families can be found by this way but also well-known orbit families such as Sun-synchronous orbits, Molnija-orbits, Tundra-orbits and many others can be in a complementary way examined from this aspect. In a general point of view, we can conclude: the consideration of equivalence orbits offers a very special but fascinating insight in the extremal wide field of astrodynamics.

Of course there are many other aspects to consider those orbit families as induced by higher physical impacts. This is correct for low orbits respecting the influence of the solar flux as well as the high order gravitational field of the Earth (e.g. the geodetic satellites Champ, Goce, Grace [15], etc.]), or for high altitude orbits and the impact by the influence of interplanetary as well as interstellar effects. A typical example of a special point of view on the motion of an Earth satellite is the Earth Moon. In mathematical sense the Moon can be considered as an Earth satellite. However in physical sense the Moon never moves "around" the Earth. Its path is outside the attraction sphere of the Earth, but inside the activity sphere [13,14]. Therefore the path of the Moon is always concave oriented towards the Sun. The motion of the Moon is essentially "perturbed" by the Earth. Another aspect is the triaxiliaty of the Moons body. It influences a Moon orbiter, but it can also influence the motion of a high altitude (and nearly circular) orbit of an Earth satellite.

Declaration of competing interest

The authors declare that they have no known competing financial interests or personal relationships that could have appeared to influence the work reported in this paper.

Acknowledgments

The author cordially thanks *Dipl. Ing. Mark Lützner* for his valuable support in the compilation of this paper, to the editor and the reviewers for their careful and constructive review, and he is indepted to the director of the Microwave and Radar Institute of DLR, Prof. Dr. Ing. habil. Alberto Moreira, and the department head Dr. Ing. Thomas Neff for the support of my work by the use of the institute's infrastructure and computers.

References

[1] D. Brouwer, Solution of the problem of artificial satellite theory without drag, Astron. J. 64 (1959) 378–397.
[2] V.A. Brumberg, Analytical Techniques of Celestial Mechanics, Springer-Verlag, Berlin, Heidelberg, New York, 1995.
[3] Michel Capderou, Satellites, Orbites et Missions, Springer-Verlag France, 2003, ISBN 2-287-59772-7.
[4] A. Danjon, *Astronomie Générale, Astronomie Sphérique et éléments de Mécanique Céleste*, Seconde Edition, revue et corrigée, Librairie Scientifique et Technique Albert Blanchard, vol. 9, Rue de Médicis, Paris, 1980, p. 75006.
[5] P.A. Hansen, Auseinandersetzung einer zweckmäßigen Methode zur Berechnung der absoluten Störungen der Kleinen Planeten, erste Abhandlung', Abhandlungen der mathematisch-physischen Classe der königlich sächsischen Gesellschaft der Wissenschaften, dritter Band, bei S. Hirzel, dritte Abhandlung im fünften Band, Leipzig, 1857, p. 1861.
[6] E.F.M. Jochim, The significance of the Hansen Ideal Space Frame, Astron. Nachr./ Astr. Notes 333 (No. 8) (2012) 774–783, https://doi.org/10.1002/asna.202222711.
[7] E.F.M. Jochim, *Satellitenbewegung, Band IV, Bewegungsanalyse* (Satellite Motion, vol. IV.: Satellite Orbit Analysis), ISRN DLR FB 2018–31 (2018). ISSN 1434-8454.
[8] P.K. Seidelmann (Ed.), *Explanatory Supplement to the Astronomical Almanac*, A Revision to the Explanatory Supplement to the Astronomical Ephemeris and the American Ephemeris and Nautical Almanac, Prepared by the Nautical Almanac Office, U. S. Naval Observatory with Contributions from H. M. Nautical Almanac Office, Royal Greenwich Observatory, Jet Propulsion Laboratory, Bureau des Longitudes, and the Time Service and Astrometry Departments, ed., U. S. Naval Observatory, University Science Books, Mill Valley, California, 1992, ISBN 0-935702-68-7.
[9] K. Stumpff, Himmelsmechanik III, DVW Berlin, 1974.
[10] M.C. Eckstein, Ein Satellitenbahnmodell ohne Singularitäten', DLR-FB 73-67, 'A Satellite Model without Singularities, ESRO TT-102, 1973. Oct. 1974.
[11] Sean E. Urban, P. Kenneth Seidelmann (Eds.), Explanatory Supplement to the Astronomical Almanac, (eds.)third ed., University Science Books, Mill Valley, CA, 2013, ISBN 978-1-891389-85-6.
[12] E.F. Jochim, The Synodic Motion of Satellites Related to Sun'. *Proceedings Of the AAS/AIAA Astrodynamics Conference*, Lake Placid, New York, 1983. August, 22 - 25, 1983. AAS 83-334.
[13] E.F.M. Jochim, *Satellitenbewegung, Band III, Natürliche und gesteuerte Bewegung* (Satellite Motion, Vol. III.: Natural and Guided Motion), ISRN DLR FB 2014–36 (2018 b). ISSN 1434-8454.
[14] W. Schulz, Über Einflussbereiche von Himmelskörpern, Z. für Flugwiss. Weltraumforsch. 1 (1977) 365–375.
[15] http://podaac.jpl.nasa.gov/grace/data_access.html#Level2.